Investigating the ecological basis of divergent visual evolution between two Heliconius butterflies

Master's Thesis by Léo Laborieux

Submitted March 1st, 2024

Supervisors :
Prof. Dr. Richard Merrill
José Borrero



MEME

EES LMU
MUNICH GRADUATE PROGRAM FOR EVOLUTION, ECOLOGY AND SYSTEMATICS

LMU
LUDWIG-MAXIMILIANS-UNIVERSITÄT MÜNCHEN

Abstract | Ecological speciation depends on a source of divergent selection between incipient species. As such, environmental heterogeneity may foster local adaptation in important sensory traits, driving reproductive isolation. In a putative response to distinct local vegetation densities, some phylogenetically close pairs of *Heliconius* butterflies are known to exhibit adaptive differences in visual acuity, a trait that may influence survival and reproduction. However, the exact ecological underpinnings of their visual evolution remain unclear. I investigated the relationship between spatial complexity and behaviour in *H. cydno* and *H. melpomene*, two sister taxa with marked differences in visual acuity, and quantified the complexity of their natural habitats. I found that the habitats of both species differed in canopy cover, but not in understorey congestion, suggesting an important role of flight height in modulating experienced levels of spatial complexity. Common-garden experiments involving live individuals revealed higher absolute activity levels in *H. melpomene*, but no discernible differences in how both species responded to changes in spatial complexity. This latter pattern held true across various ecological contexts, including exploratory behavior, obstacle avoidance, mate choice, and oviposition. Recommendations are given for future studies.

I. Introduction

During ecological speciation, ecologically-based divergent selection between environments drives population divergence until the formation of distinct species (Nosil, 2012). Understanding when and how ecological selection can lead to the interruption of gene flow is critical, and exploring the potential of sensory adaptation to underlie ecological speciation represents an important way to address this question (Endler, 1992; Boughman, 2002; Maan et al., 2006). Indeed, incipient species often use different microhabitats (Rice, 1987), exposing them to contrasting sensory environments. This may foster adaptive divergence in sensory systems, since accurate perception of the surrounding environment is crucial for survival and efficient resource exploitation in the wild. In turn, this form of local adaptation may promote speciation (Nosil, 2012).

Habitat specialization through sensory adaptation can contribute to both pre and post-mating isolation. Premating isolation due to differences in sensory ecology are most often thought to evolve as a result of sensory drive (Endler, 1992), where distinct sensory environments can influence female sensory characteristics and preferences, fostering divergent shifts in male signaling and, eventually, reproductive isolation. However, pre-mating isolation may also evolve due to immigrant unviability (Nosil, 2012), where incoming migrants are suitably adapted to their habitat of origin but not to the environment they are entering. Differences in sensory ecology may also result in post-mating isolation due to a decrease in hybrid fitness, where hybrids display intermediate traits mismatched to the ecological optima of either habitat. While sensory drive has been investigated in a number of study systems with variable support (Maan et al., 2006; Seehausen et al., 2008; Cummings & Endler, 2018), demonstrations of a causal relationship between local sensory adaptation and speciation that do not involve sensory drive-like processes remain rare (but see Maan et al. (2017)).

The nymphalid *Heliconius* butterflies display complex visual systems, a characteristic broadly attributed to their ecology. Remarkably, members of the genus evolved some of the largest heads and eyes of any neotropical butterflies (Seymoure et al., 2015), representing an intriguing level of investment in vision. This high investment is likely due to a combination of biotic and abiotic pressures. On the one hand, the bright warning patterns of *Heliconius* butterflies balance a dual role as both mimetic predator deterrents and mating cues, influencing visual evolution. *Heliconius* butterflies are often involved in Müllerian mimicry rings (Müller, 1879), and their vision appears to have evolved alongside their wing pigments to minimize confusion induced by comimics during mate search (Bybee et al., 2012; Dell'Aglio et al., 2018). On the other, the highly contrasting visual environments of certain ecologically distinct species pairs (Estrada & Jiggins, 2002) predict that *Heliconius* visual evolution may also be driven by the abiotic environment. Significant adaptive differences in the visual systems of

ecologically distinct species pairs (Seymoure et al., 2015; Montgomery & Merrill, 2017; Montgomery et al., 2021; Wright et al., *in review; Wright et al., unpublished data*) support this prediction. However, the exact ecological pressures driving visual evolution remain unknown.

Heliconius cydno and *Heliconius melpomene* are closely related species, with a divergence time of approximately 1.5 Ma (Mallet et al., 1998; Beltrán et al., 2002). These two Central and South American butterflies are divergent in colour pattern, host preferences and habitat preferences (Estrada & Jiggins, 2002; Merrill et al., 2013). Previous work (Estrada & Jiggins, 2002) shows that, in Panama, *H. melpomene* occupies relatively open secondary forests and forest edges, while *H. cydno* apparently favours closed-canopy forest environments. Despite these distinct habitat preferences, populations of both species are often organized in "mosaic" sympatry following local vegetation. Interspecific contacts are frequent, but hybridization is rare (<0.1%, Mallet et al. (1998b)).

H. cydno and *H. melpomene* differ in their visual acuities. Specifically, optomotor assays show that *H. cydno* displays higher visual acuity, in both sexes, compared to *H. melpomene*, with a greater gap in males (J. Borrero et al., *unpublished data*). These differences in eye resolving power appear to be underpinned at least partially by eye morphology, *H. cydno* possessing larger eyes with higher ommatidia counts, and larger ommatidiae altogether (Seymoure et al., 2015; Wright et al., in review). Importantly, evidence points to ommatidia count and corneal area having diverged under selection (Wright et al., *in review*). This combined evidence suggests that the emergence of distinct levels of visual acuity may represent local ecological optima for navigation in variably complex environments. However, understanding whether and how this instance of local adaptation may have contributed to ecological speciation requires identifying the drivers of visual evolution in these species. To date, no study has explicitly investigated the ecological selective pressures acting on *Heliconius* visual acuity, let alone in *H. cydno* and *H. melpomene*, warranting further investigation.

Here, I aim to characterize the ecological basis for divergent visual acuity evolution in *H. cydno* and *H. melpomene*. I focus on assessing (i) whether the natural microhabitats of both species exhibit quantitative differences in spatial complexity and (ii) whether the two taxa show distinct behavioural responses to local variation in spatial complexity. To address this first question, I ran photographic surveys in the wild, and recorded behavioural and morphological data for wild individuals. To investigate the second, I conducted over 150 experimental trials involving captive-bred individuals of both species, examining the variation of activity levels, oviposition preferences and male courtship across distinct environments. I also attempted, for the first time, to directly quantify the relationship between navigational performance and spatial complexity using directed movement and a variable-speed rotary obstacle.

II. Materials and methods

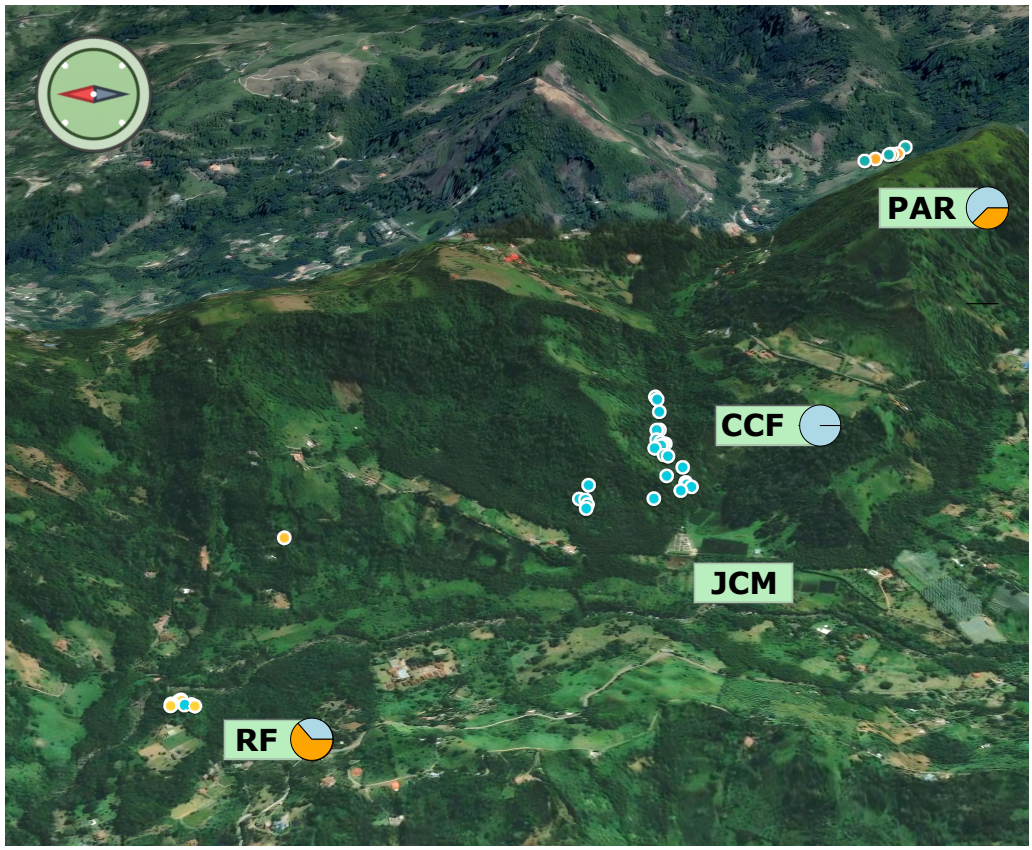


Figure 1 | East-oriented topographic map of the sampled localities. JCM: José Celestinos Mutis research station. CCF: closed-canopy forest. RF: riparian forest. PAR: Paraiso Andino reserve. Blue represents *H. cydno* and orange represents *H. melpomene*. Pie charts indicate the proportions of both species sampled per locality.

II.1 | Field experiments

II.1.1 | Butterfly sampling

All wild butterflies used for data collection originated from localities in the close vicinity of Universidad del Rosario's José Celestino Mutis (JCM) research station in La Vega, Cundinamarca, Colombia ((4.955836, -74.381466), Fig. 1). Both *Heliconius melpomene* and *Heliconius cydno* occur natively in the area. In total, three localities were sampled : (i) a patch of closed-canopy temperate rainforest located on the research station's property ((4.955617, -74.379642); ~1350m a.s.l), (ii) the edge of a riparian forest ((4.964609, -74.383777); ~1250m a.s.l) and (iii) within the Paraiso Andino reserve ((4.949072, -74.370015); ~1500m a.s.l). I recorded individual data for all collected butterflies,

including species, morphotype (for *H. cydno*: white or yellow wings), sex, time and date of capture, pollen load, total body length and flight height. Pollen load was assessed categorically, characterized as (i) no pollen, (ii) some amount of pollen below apparent saturation of the proboscis or (iii) apparent proboscis saturation. Flight height was recorded as observed when individuals were first spotted, using a butterfly net handle of known length or a measuring tape, following recommendations by Dell'Aglio et al. (2022). This dataset (Table S1) will mainly contribute to other projects, although flight height is treated in this study.

II.1.2 | *In-situ* characterization of habitats

I assessed spatial complexity at the localities sampled for wild butterflies using photographic data. Each butterfly was given a unique identifier and geotagged using the Organic Maps application on an Apple iPhone 12 Mini smartphone. For each unique capture site, photographic data was acquired exactly where the individual was collected, or within a 5-meter radius when conditions did not allow for better accuracy. Sites were defined as unique when their 5-meter radia did not overlap. Photographs were taken using a Fujifilm X-Pro 3 digital camera equipped with a 23mm ƒ/2 lens, corresponding to a horizontal angle of view of approximately 37°. The camera's output mode was set to RAW, enabling higher post-processing flexibility, and the lens aperture was set to ƒ/8 to maximize detail rendition. For data collection, a square, white fabric sheet (2.4m*2.4m) was hung and tensioned between nearby vegetation, acting as a bright backdrop against which the darker vegetation was easily discriminated. Photographs were taken at a standardized distance of 3 meters, in front of and behind the sheet, before rotating the latter 90° along one of its two anchor points. After rotation and re-anchoring, two more photographs were taken, front and back, for a total of four ground-level photos (Fig. 2). Vegetation obstructing the camera's field of view at a distance lower than 50cm was removed, to avoid disproportionate blockage. All photographs were taken at eye level, following local terrain features. Additionally, a final photograph was taken of the canopy, holding the camera perpendicular to the ground.

Photos were imported as RAW files to Capture One 21 for initial post-processing. Files were initially converted to black and white, then cropped to the area obstructed by the sheet. Both global and local adjustments were then applied to increase the contrast between the vegetation and the white backdrop. This is a necessary step because the tonal ranges of the sheet and bright areas of the foliage may sometimes overlap in unprocessed images. Pre-processed photographs were exported as JPEG files with maximum quality settings before being imported into ImageJ 1.53t (Schneider et al., 2012), where they were converted to binary colours (i.e. black or white). After careful masking of the

sheet's outline, including potential folds and bent edges ("Polygonal selections" tool), a threshold analysis yielded the proportion of black pixels in the selected part of the image, i.e. the relative area on the sheet being obstructed by vegetation. Canopy photographs were directly converted to binary and subjected to threshold analysis, effectively isolating canopy elements from the sky.

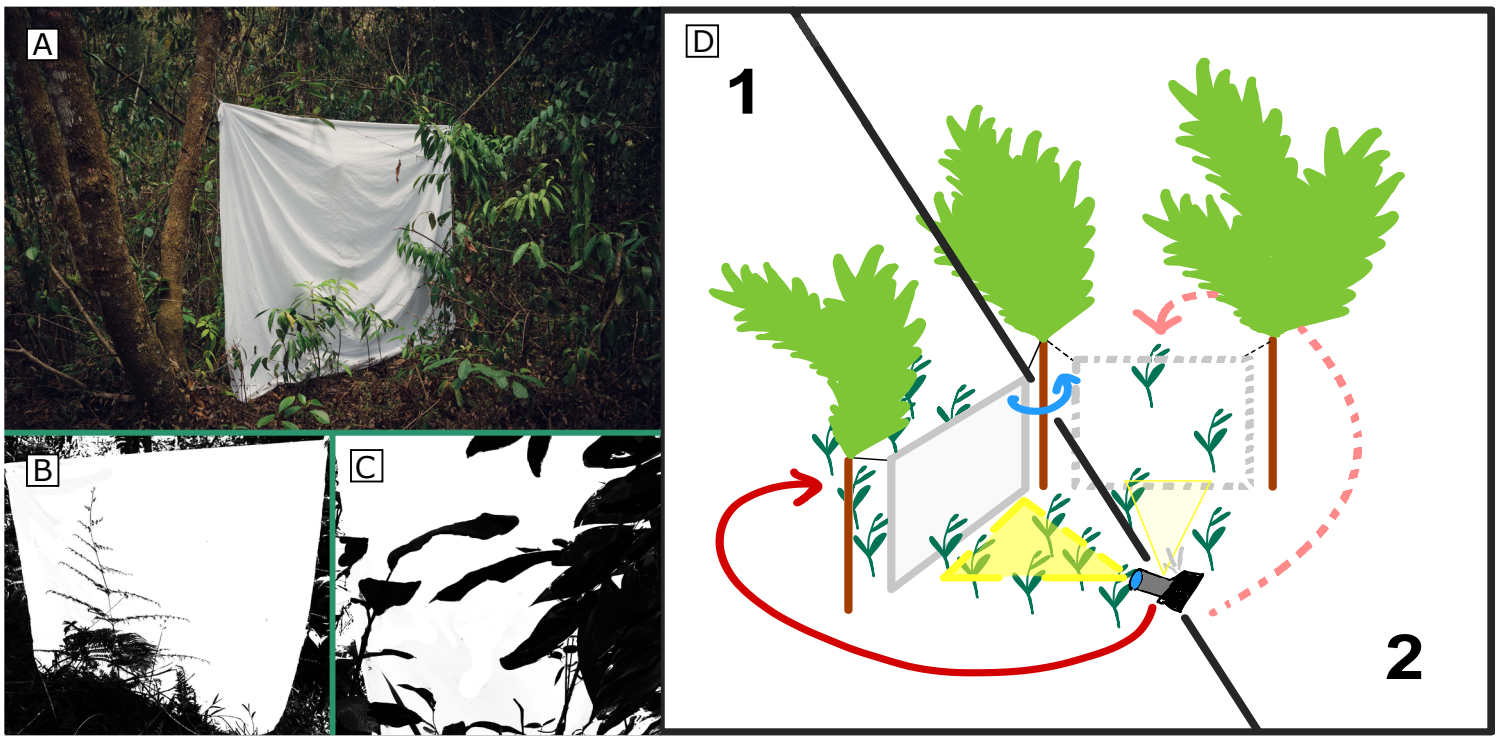


Figure 2 | Vegetation-induced blockage. A: data collection apparatus (side view). B: processed image from a typical *H. melpomene* capture site. Front view, but with suboptimal tensioning of the sheet, requiring masking during ImageJ processing. C: processed image from a typical *H. cydno* capture site. Front view with optimal tensioning of the sheet. D: experimental setup. Phase 1 (left): the sheet is tensioned and photos are taken, front and back. Phase 2: the sheet is rotated 90° along one of its anchor points, and a second pair of photos is taken (front + back).

II.2 | Insectary experiments

II.2.1 | Butterfly rearing

All butterflies used for experiments were bred and reared at the JCM experimental station under common garden conditions, mitigating the potential influence of environment-induced developmental plasticity. Butterflies were kept in groups in 1m x 2m x 3m insectaries (W x H x L). All adults had constant access to a pollen-sucrose solution and blooming *Lantana* plants. Adult females were allowed to deposit eggs on *Passiflora monolobada* and *Passiflora trilobada* plants, and these eggs were collected daily. Larvae hatched from these eggs were fed on *P. monolobada* in the laboratory until pupation, while those that hatched within the insectaries themselves remained free

to feed on both *Passiflora* species. The proportions of lab-reared and cage-reared individuals was roughly equivalent between species.

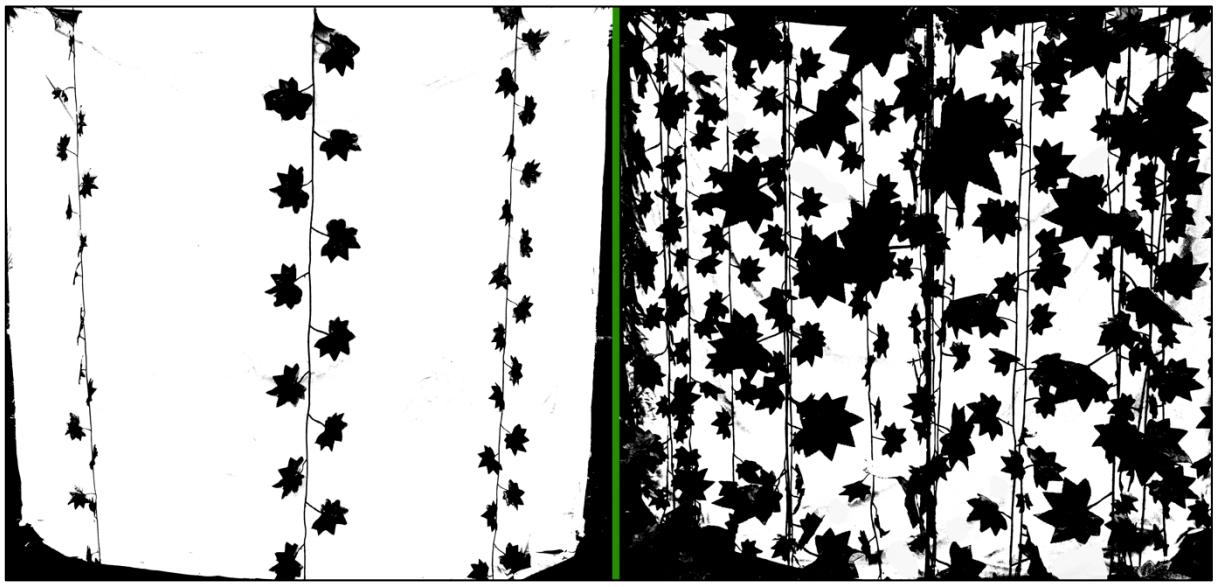


Figure 3 | Vegetation-induced blockage in the simple (left, 6% obstruction) and complex (right, 49% obstruction) experimental insectaries arranged for the exploratory activity experiment.

II.2.2 | Exploratory activity and spatial complexity

Experimental insectaries were set up to investigate, in both species, relative exploratory activity across distinct levels of spatial complexity. These larger insectaries (2m x 3m x 2m) contained vertical vine-like plastic plants (leaves approx. 10cm in diameter), hung from the ceiling, with all real plants removed. Spatial complexity was modelled as the concentration of vines in the insectaries and categorized into two levels — one simple and one complex. The vine densities corresponding to “simple” and “complex” environments were approximately 0.8 and 3,3 vines per square meter, respectively. Blockage analysis as described above results in estimates of 6% obstruction for the “simple” treatment and 49% obstruction for the “complex” treatment (Fig.3). The complex vine arrangement therefore satisfactorily emulated understorey conditions in the wild habitats of both species (see Results section), while the simple treatment corresponded to a significantly more open environment. To mitigate the effects of spatial variation in local conditions, the two trial insectaries were chosen to be as physically close to each other as was feasible.

To score the exploratory activity of the butterflies, the space encapsulated by the insectaries was divided into four equal quadrants, themselves delimited by a vertical projection of the roof's

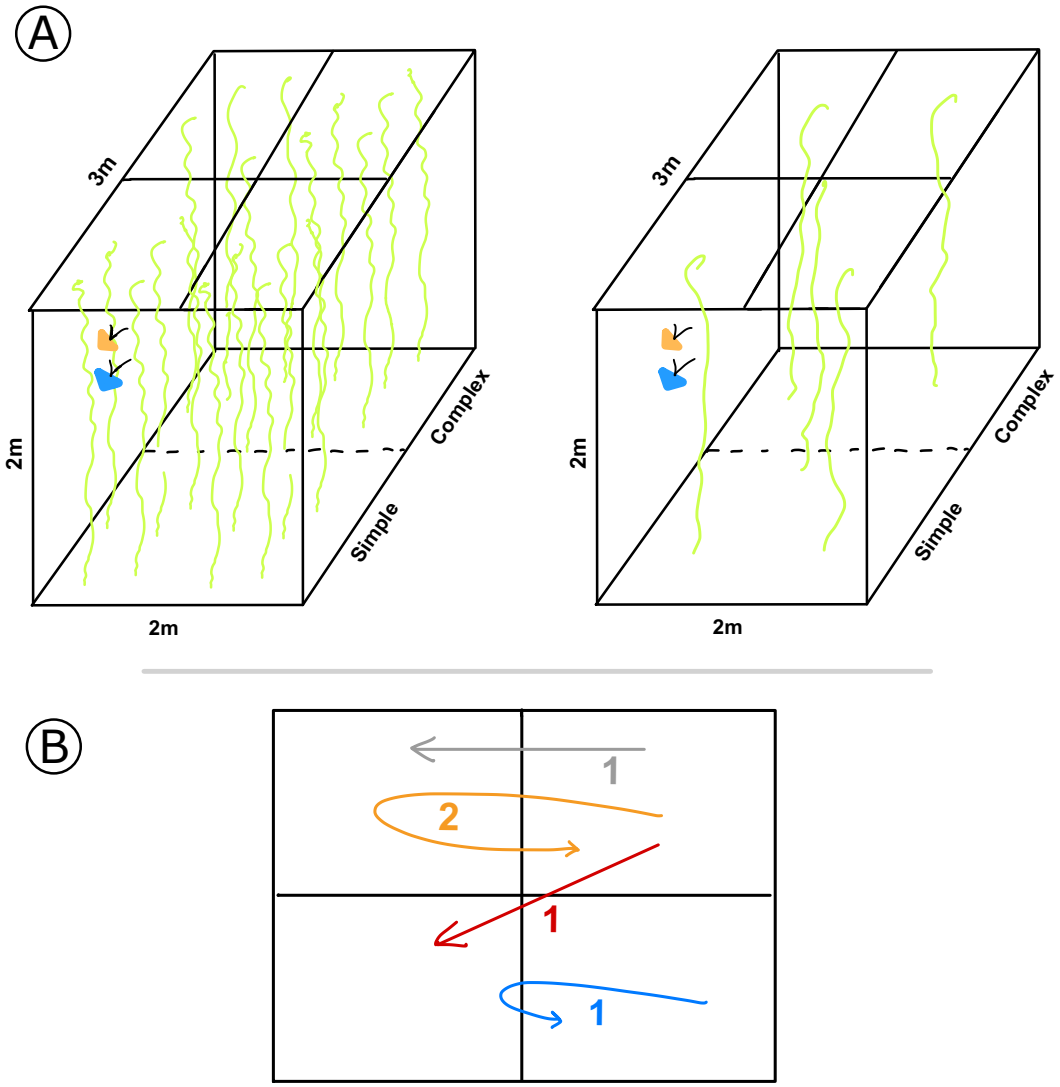


Figure 4 | Butterfly exploratory activity experiment. A: two pairs of males (blue: *H. cydno;* orange: *H. melpomene*) are tried concurrently, with one insectary set up as a complex environment (left), and the other as a simple environment (right). B: scoring system based on movement type (arrows). Numbers indicate the scores obtained for each movement type.

cross-shaped metallic structure (Fig. 4)**.** Individuals scored one point when entering a new quadrant. To avoid overestimates, individuals crossing the insectary diagonally only scored one point. Similarly, individuals that briefly intruded the edge of a new quadrant before quickly flying back only scored one, since this did not reflect long-distance movement. Butterflies crossing quadrant edges while walking did not score points. Both insectaries were shaken simultaneously every five minutes to

encourage movement, unless this would lead to a loss of data on the part of the observer (i.e. unless high activity was already being recorded).

Males of both species were tested between September 15 and October 4, 2023, where experimental sessions took place between 10am and 2pm. Trial groups were comprised of four individuals: two *H. melpomene* and two *H. cydno*. These groups were randomly subdivided into pairs comprising one male of each species, and these pairs were randomly assigned via dice roll to the simple or complex insectaries, respectively. Trials lasted twenty minutes, while the exploratory activity of each individually identified butterfly was recorded. After a first twenty-minute trial, both pairs of males were permutated between the two insectaries for a second trial in the treatment that the butterflies had not yet experienced. The weather was recorded for each trial and categorized into three levels: sunny (<50% cloud cover), cloudy (>50% cloud cover) or overcast (100% cloud cover). No trials were conducted on heavily overcast or rainy days, which were unsuitable for data collection due to low butterfly activity. The treatment types (complex or simple) were also permutated after half of the data collection period had elapsed, to further control for the potential fixed effects of local conditions.

II.2.3 | Habitat preference for oviposition

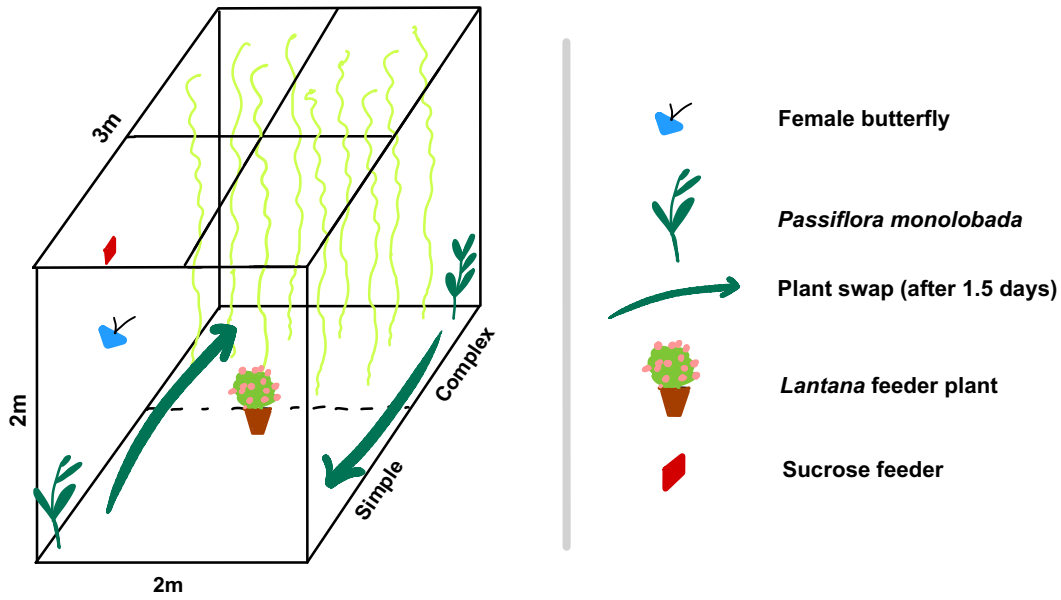


Figure 5 | Oviposition experiment. Blue: *H. cydno*. Orange: *H. melpomene*. The simple side of the insectary (front) is drawn without vines for readability. Vine density on complex side (back) not representative.

To investigate the relationship between species, local spatial complexity and oviposition behaviour, I evaluated oviposition preferences for spatially complex or simple environments in both species. Two 2m x 3m x 2m insectaries were divided into two sections of equal area, one complex and one simple, along their length. Simple and complex environments were defined in two ways over the course of the data collection period (hereafter "vine setups"): simple and complex initially followed the same vine density characteristics as in II.2.3, but later increased to 3,3 vines/m^2 and 6.6 vines/m^2, respectively. To control for the potential fixed effects of cage orientation, the simple side was oriented northward in one cage, and southward in the other. In each cage, female butterflies were provided with sucrose solution and a single, flowering *Lantana* plant. Plants occupied opposite angles in the insectaries (Fig. 5).

Trials lasted three full days, divided into two equal periods. Single females were randomly assigned to one of the two experimental insectaries and resided there for a day and a half. Eggs were then collected in both parts of the cage, and the plants were swapped across treatments. The plant swap was performed to avoid probable plant-specific effects, where oviposition attractiveness differed slightly between plants. The butterflies were allowed to reside in the insectaries for another day and a half, until the end of the third day. Eggs were collected a second time at the end of the trial, when the butterflies were removed. The total numbers of eggs laid in the simple and complex areas of the insectary were then summed separately.

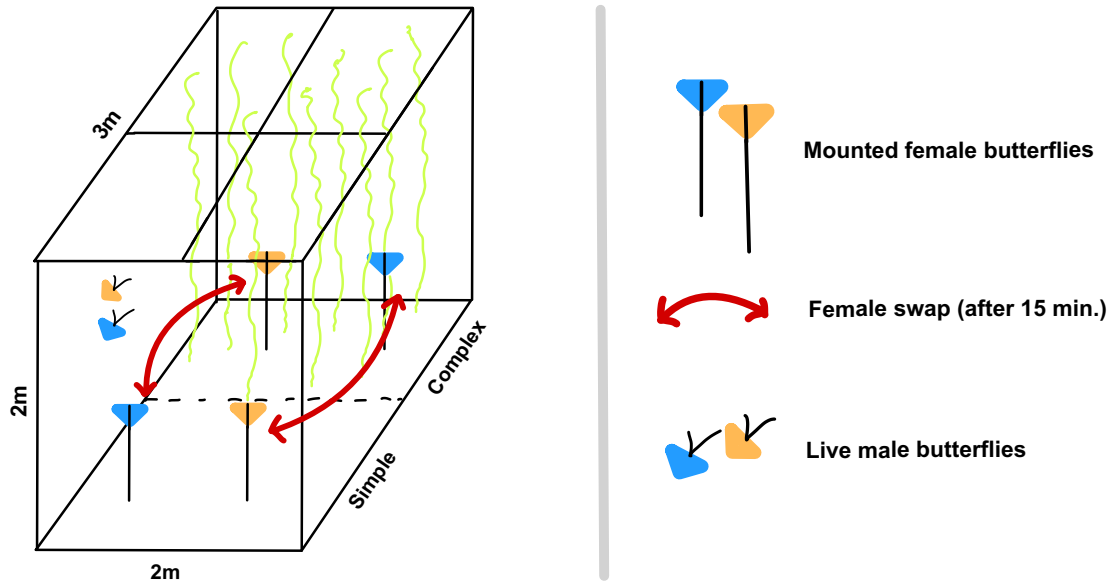


Figure 6 | Mate choice experiment. Blue: ***H. cydno***. Orange: ***H. melpomene***. **The simple side of the insectary (front) is drawn without vines for readability. Vine density on complex side (back) not representative.**

II.2.4 | Mate search performance and spatial complexity

To investigate whether the distinct levels of visual acuity exhibited by both *Heliconius* species induced behavioural differences in mate search and courtship, males of *H. cydno* and *H. melpomene* were placed in another 2m x 3m x 2m insectary with mounted females. This insectary was divided along its length into a simple section and a complex section, similar to the setup outlined in II.2.3. Vine densities were set to 0.8 vine/m^2 and 3,3 vines/m^2, and no food sources were introduced. Females of both species were collected and washed in dichloromethane for 5 minutes to eliminate all wing pheromones, and isolate visual signals (for methodology, see Hausmann et al. (2021)). The butterflies were then glued to thick wire and placed in both environments within the insectary at standardized positions (Fig.6), 130cm above ground. The configuration in which the females were placed was constrained (i.e. one female of each species along both the length and width of the insectary), but nonetheless randomized.

Males were tried in pairs (one of each species) over 30-minute trials between November 8, 2023 and January 18, 2024. Intraspecific and interspecific courtship attempts (hovering) were recorded throughout. Trials were divided into two 15-min periods between which females were permutated across treatments to avoid female-induced fixed effects. To better represent courtship duration, trials were further partitioned into 60-second intervals during which behaviour was either observed and recorded or absent (see Rossi et al., *in press* (2024)). This data structure also enabled recording of the time elapsed (latency) to first courtship in both environments, and for both males. For individuals that did not attempt courtship, latency to first courtship was set to 30 minutes. Intraspecific and interspecific courtship were recorded separately. The insectary was shaken every 3 minutes to stimulate butterfly activity.

II.2.5 | Obstacle avoidance

In order to further investigate the effect of spatial complexity on navigational performance, butterflies of both species were stimulated to fly through a variable-speed rotary obstacle. A 2m x 3m x 2m insectary was divided lengthwise into two equal sections. The roof and sides of the first section were entirely obstructed by light-tight tarp, while the second section remained unblocked, creating a strong light gradient. The light and dark halves of the insectary were separated by an opaque tarp divider interrupted in its center by a vertical 60-cm slit. The slit contained a variable-speed rotary obstacle, motorized by a modified optomotor machine attached to the roof armature of the insectary (Fig. S1). The rotary obstacle was composed of 12 equally spaced artificial vines hanging vertically, and fastened

to two circular frames at their extremities. The resulting tubular obstacle was allowed to spin between 3 and 18 RPM, as controlled by an Arduino microcontroller. Individuals were released from a fixed point situated at the back of the dark chamber, in mid-air, enabling measurement of their traversal times.

In this experiment, I used rotation speed as a proxy for spatial complexity. Accordingly, male butterflies were tested at the two extremes of the speed range allowed by the motor (3 and 18 RPM), with three replicates per individual and per treatment. Time to cross was measured using a stop watch, starting at the release of the butterfly. The chronometer was stopped once the individual left the outer perimeter of the spinning obstacle, on the light side of the insectary. Butterflies that landed on the obstacle or flew under it, instead of crossing, were retried. Butterflies that landed elsewhere in the dark chamber before crossing were also retried. The trial group was subjected to one treatment, slow or fast, before being collected in the light chamber and tried again at the other spinning velocity. This sequence was repeated three times. Temporal variation in sunlight intensity affected the luminosity gradient between the dark and light chambers. To mitigate this effect, the butterflies were tried in quick succession while alternating species.

II.3| Statistical analyses

Statistical analyses were conducted in R (R Core Team, 2023) and plots were created using the *ggplot2* package (Wickham, 2011).

Spatial complexity in the wild. Obstruction caused by vegetation was derived from continuous quantities as recorded by photographic data. These data were thus modeled via beta regression, as recommended by Douma & Weedon (2019). Using the *glmmTMB* function of the glmmTMB package (Brooks et al., 2017), I fitted a generalized linear-mixed model GLMM following a beta distribution and tested the influence of species (the only fixed effect) on vegetation-induced obstruction in the understorey. To avoid pseudoreplication, locality (PAR/RF/CCF) was included as a random effect. The minimum adequate model was identified by using likelihood ratio tests (LRT) (Crawley, 2002) as implemented in the function *drop1*. The significance of the fixed effect of species was assessed using the *Anova* command of the car package (Fox & Weisberg, 2019). The canopy cover dataset, in contrast, was four times smaller by design (*melpomene*: n=10; *cydno*: n=32) and canopy cover proportions were analyzed using a Wilcoxon signed-rank test. An identical test was performed on the understorey dataset for comparison purposes.

Flight height. To test whether flight height differed between species, I fitted a mixed-effect linear model to the field-collected dataset using the *lmer* function of the lme4 package (Bates et al.,

2015). This model included species as the only fixed effect, and locality was once again included as a random factor. Model selection was performed as for the obstruction data.

Exploratory activity. For the experiment investigating exploratory activity, I fitted a negative binomial GLMM using the *glmer.nb* function of the lme4 package and tested how butterfly activity score was influenced by (i) species, (ii) treatment (simple / complex), (iii) their interaction and (iv) weather (<50% cloud cover / >50% cc / 100% cc). The dependent variable representing activity was the activity score determined from between-quadrant movement. Because butterflies were tested multiple times, individual ID was included as a random factor to avoid pseudoreplication. To account for potential interactions between individuals, trial group (i.e. four individuals tested simultaneously) was included as a second random factor. Model reduction was then performed stepwise via *drop1*, and the significance of the fixed effects was assessed using parametric bootstrapping via the package pbkrtest (nsim=10, Halekoh & Højsgaard, 2014).

Oviposition. For the oviposition experiment, I tested whether preferences for either oviposition environment (simple/complex) differed between species. I fitted a binomial GLMM with *glmer*, testing how the number of eggs laid in the simple/complex areas of the insectaries was influenced by the fixed effects: (i) species, (ii) vine setup (low / high density) and (iii) their interaction. Individual ID was once again included as a random factor to account for occasional female re-uses. Location was included as an additional random factor, since data was collected in two separate insectaries. Model reduction and selection was performed as for the activity experiment.

Mate choice. A similar analysis was conducted for the mate choice experiment. A binomial-distribution GLMM was fitted to the data to test how the number of courtship attempts in the simple/complex areas of the insectary was influenced by the fixed effects: (i) species, (ii) orientation of the cage (complex area on northern or southern side), (iii) their interaction and (iv) weather. Individual ID was included as a random factor. Model selection followed the methodology described for the activity and oviposition experiments, and the significance of fixed effects was assessed using the *Anova* command.

Obstacle avoidance. Finally, I fitted a mixed-effect linear model to assess the impact of rotation speed on the obstacle traversal capabilities of both species. There, obstacle traversal time was modelled with the fixed effects: (i) species, (ii) treatment (3 / 18 rpm) and (iii) their interaction. Individual ID and replicate number were included as random factors. Model reduction was performed with *drop1* and the significance of fixed effects was assessed using the *Anova* command.

III. Results

III.1 | Photographic data discriminate *H. cydno* and *H. melpomene* microhabitats based on canopy, but not understorey.

Capture sites of individual butterflies were highly clustered across the collecting area (Fig. 1). *Heliconius cydno* was collected at all three localities. *H. melpomene*, on the other hand, was only collected at the edge of the riparian forest and at the Paraiso Andino reserve (60% and 63% of all collected *Heliconius* individuals respectively), where it co-occurred with *H. cydno*. Notably, *H. cydno* appeared to be the only *Heliconius* species occurring at the closed-canopy forest (CCF) locality (Fig. 1). This contrasts with *H. melpomene*, which readily occurred in ecotones: near trails, or in generally patchy landscapeslandscape containing both forests and deforested areas of residential or agricultural nature. No other *Heliconius* species were observed or caught. Flight height of *H. melpomene* was lower on average than *H. cydno* (Anova: F=4.5148, df=1, p=0.0395, Fig. 7).

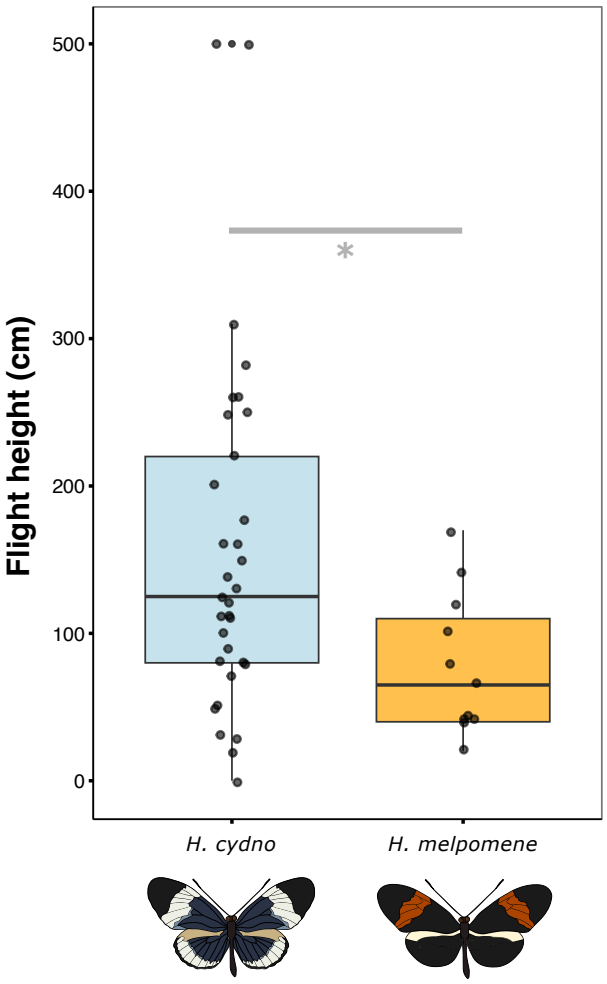


Figure 7 | *H. cydno* and *H. melpomene* significantly differed in their mean flight heights.

Photographic data was acquired at 11 total captures sites for *H. cydno*, and 8 for *H. melpomene*. In 3 occasions, individuals of both species were captured within 5 meters of each other, resulting in one unique capture site (as per the definition outlined in II.1.2). The photographs taken at these sites were included in both the *H. cydno* and *H. melpomene* datasets. There was greater canopy cover at *H. cydno* collection sites (mean = 82%) than at *H. melpomene* collection sites (mean = 53%)

(Fig 8C-D; Mann-Whitney test, W = 60, p = 0.0166). Notably, there was far greater variation in canopy cover for the *H. melpomene* collection sites (Fig 8D). There was no significant difference in understorey blockage (Fig. 8A-B). This result was obtained from both the Mann-Whitney test (W = 838, p= 0.1601) and anova on the beta-distributed GLMM (X^2 = 0,0055, df = 1 , p = 0.9407; "emmeans" contrast assessment: ß±SE = 0.0229 ± 0.308, 95% CI = -0.0182,0.0196).

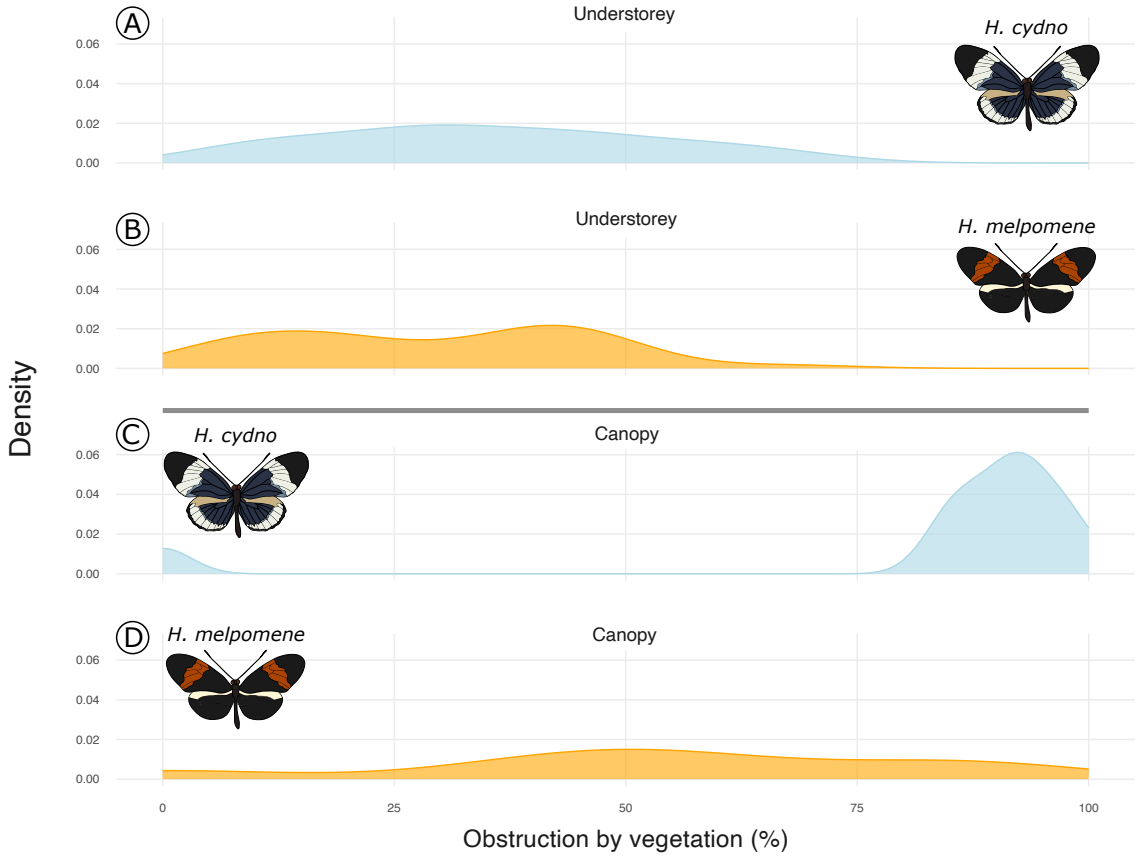


Figure 8 | Observed distributions of vegetation-induced obstruction in the habitats of *H. cydno* (blue) and *H. melpomene* (orange). A-B: understorey. C-D: canopy. A score of 100% obstruction corresponds to complete loss of line of sight at a distance of 3 meters.

III.2 | *Heliconius melpomene* shows higher exploratory activity than *H. cydno*, but there was no effect of local spatial complexity.

I found little evidence for different levels of activity between the two species as a result of habitat complexity in our exploratory activity and spatial complexity trials. Specifically, although trends in the data suggest that activity proportions between the simple and complex environments differed between species, there was no statistical support for an interaction between species and treatment

(Fig. 9**;** LRT=0.0023, df = 1, p = 0.9619). Variation in local spatial complexity therefore affected both species equally. There was, however a significant species effect, indicating that *H. melpomene* is more active than *H. cydno* (Fig. 10; LRT = 6.7283, df = 1, p = 0.0095; "emmeans" contrast assessment: ß±SE = -0.585 ± 0.223, 95% CI = -1.02,-0.148), and butterflies were more active in the simple cage (LRT = 4.296, df = 1, p = 0.0382; "emmeans" contrast assessment: ß±SE = -0.387 ± 0.187, 95% CI = -0.753, -0.0199). As expected, activity was higher in sunny conditions than with moderate (Z = -2.406, p = 0.0426; "emmeans" contrast assessment: ß±SE = -12.646 ± 5.26, 95% CI = -1.171, -0.197) or complete (Z = -2,404, p = 0.04; "emmeans" contrast assessment: ß±SE = -12.655 ± 5.26, 95% CI = -1.264,-0.131) cloud coverage, although activity did not differ between cloudy and overcast conditions (Z = 0.262, p = 0.9630; "emmeans" contrast assessment: ß±SE = 0.846 ± 3.23, 95% CI = -0.451,0.587) (Fig. S2).

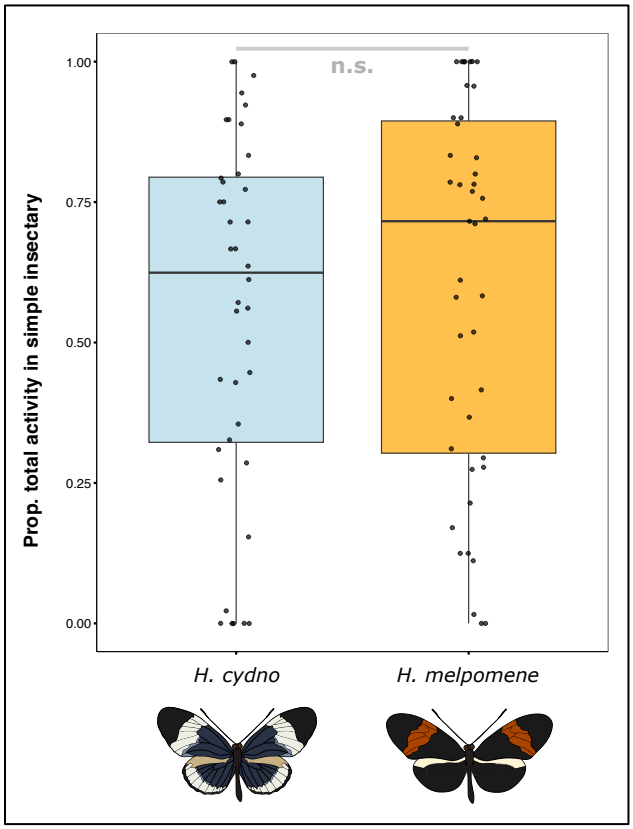


Figure 9 | The relative activity levels of *H. melpomene* (orange) and *H. cydno* (blue) did not significantly differ between the spatially simple and complex insectaries. Each point represents data recorded for one individual during one trial.

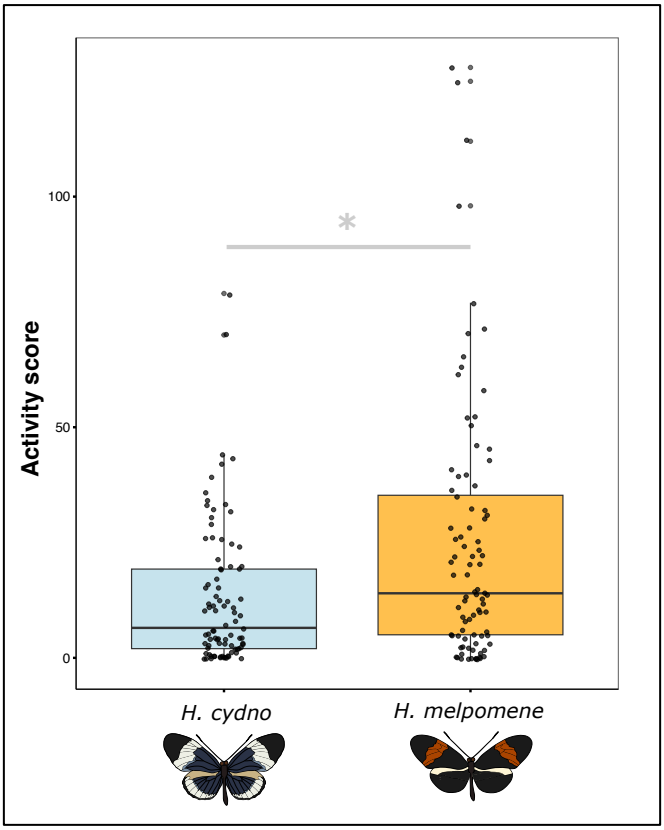


Figure 10 | *H. melpomene* (orange) was significantly more active than *H. cydno* (blue). Each point represents data recorded for one individual during one trial.

III.3 | *Heliconius cydno* and *Heliconius melpomene* do not differ in oviposition behaviour across varying levels of spatial complexity.

Data from the oviposition experiment provides little support for distinct oviposition preferences between the two species as a result of varying habitat complexities. Our data suggest that *H. melpomene* laid a larger proportion of eggs on the simple sides of the insectaries in comparison to *H. cydno* (Fig. 11). However, this was not statistically supported (LRT = 0.1405, df = 1, p=0.7078). Similarly, there was no interaction between species and vine setup (LRT = 0.9648, df = 3, p=0.8098) and, in isolation, vine setup did not have a significant effect on simple/complex proportions either (LRT = 0.8563, df = 1, p = 0.3548).

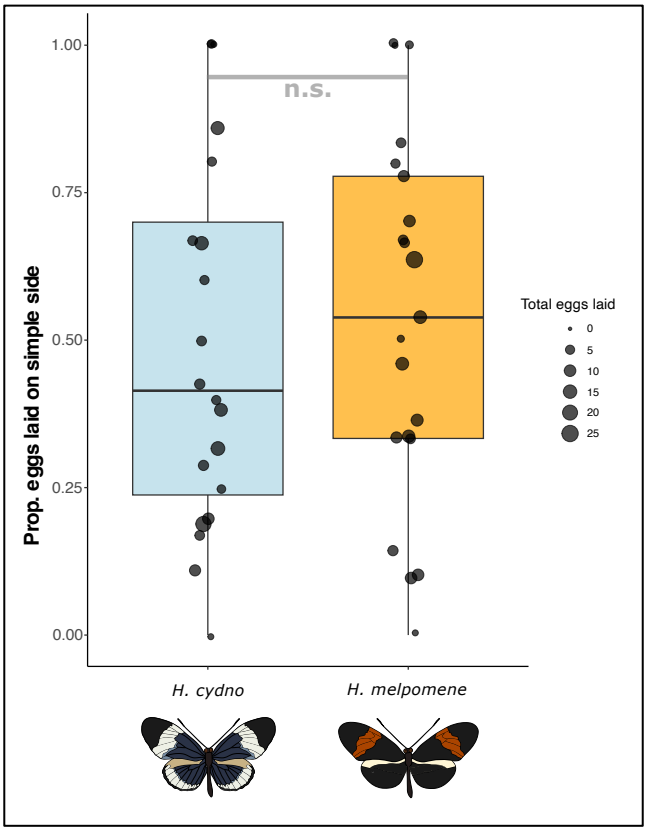


Figure 11 | The relative numbers of eggs laid by *H. melpomene* (orange) and *H. cydno* (blue) did not significantly differ between the spatially simple and complex sides of the insectaries. Each point represents data recorded for one individual.

III.4 | Latency to mate location and courtship proportions across simple and complex environments are comparable between species.

The mate choice experiments did not provide evidence for distinct patterns of courtship behaviour between the two species in response to habitat complexity. Latency to first courtship attempt did not appear to differ between species in either environment. Overall, courtship behaviour was not common (Total courtship attempts per trial per male: Mean=1,53; Median = 0; 3rd Qu. = 2.0). Because individuals that did not behave were assigned a default score of 30 minutes, distributions were largely skewed to the right (Fig. 12). This is particularly true of *H. cydno*, which did not attempt courtship as

frequently as *H. melpomene* (total courtship attempts observed for *H. melpomene*: N=222; *H. cydno*: N=54). Males that did attempt courtship did so linearly over time.

The proportion of courtship attempts in the simple and complex sides of the insectary did not differ overall between *H. cydno* and *H. melpomene* (Fig. 13; $X^2 = 3.2053$, df = 1, p= 0.0734), nor were they influenced by the orientation of the cage (i.e. simple side facing North or South) in isolation ($X^2 = 0.299$, df = 1, p= 0.5844). There was, however, a significant interaction between species and cage orientation ($X^2 = 4.6562$, df = 1 , p = 0.03094). This indicates that the effect of cage orientation differed between species, with noisy but opposite trends between *H. cydno* and *H. melpomene* (Fig. 14). Pairwise post-hoc tests further show that the sides on which both species preferred to court significantly differed in one cage orientation (Simple side = North, Z = 2.724, p = 0.0327) but not in the other (Simple side = South, Z = -0.585, p = 0.9366), suggesting that courtship was influenced by the spatial orientation of the insectary.

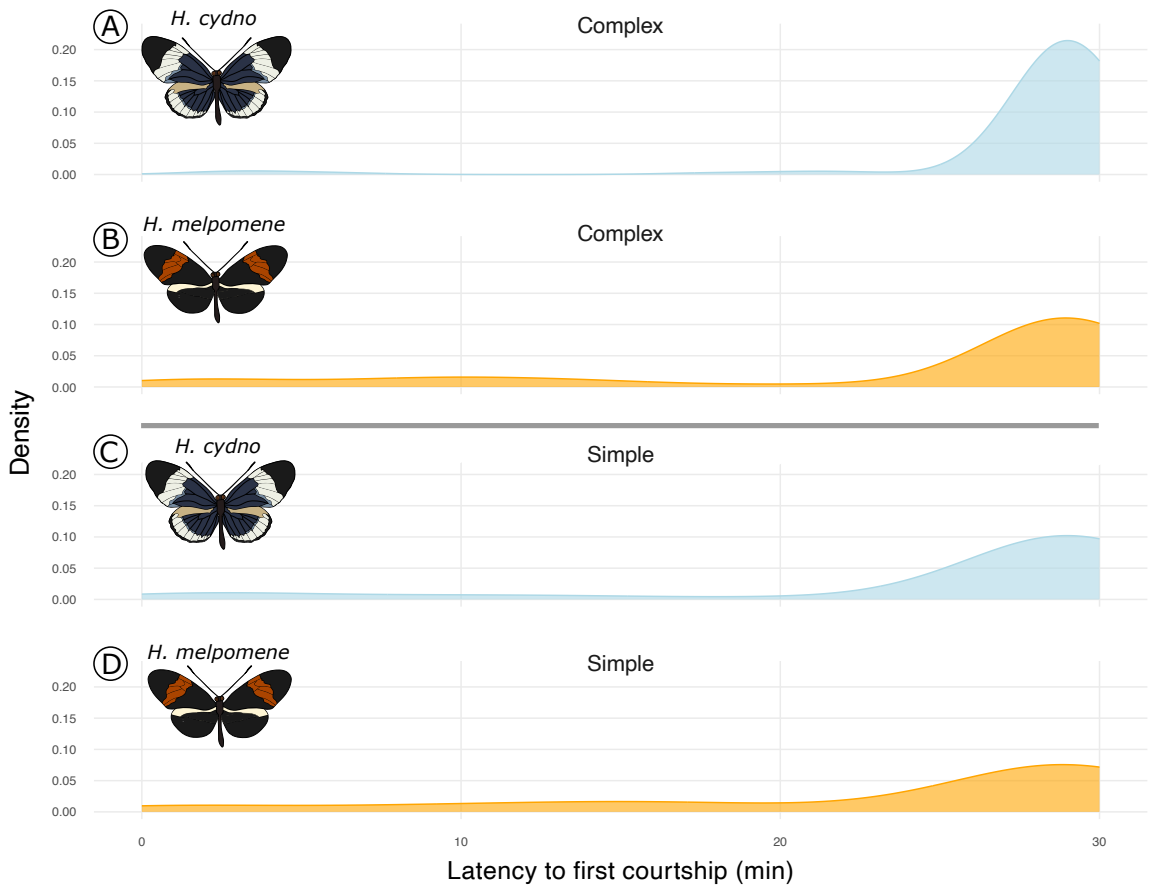
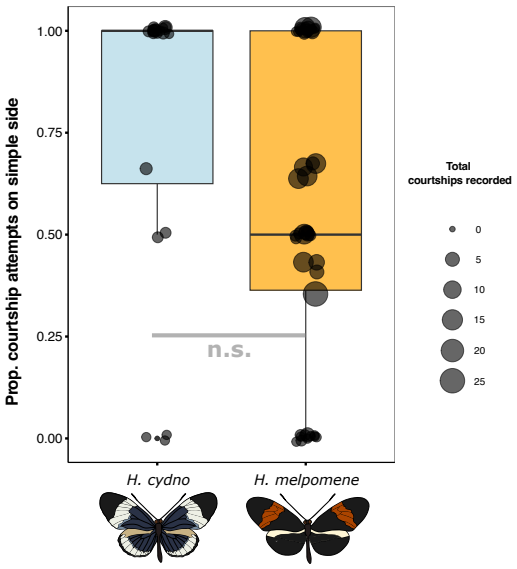


Figure 12 | Time to first courtship attempt by males of *H. cydno* (blue) and *H. melpomene* (orange). A-B: on the complex side of the insectary. C-D: on the simple side of the insectary. Individuals that did not attempt courtship were assigned a default score of 30 minutes.



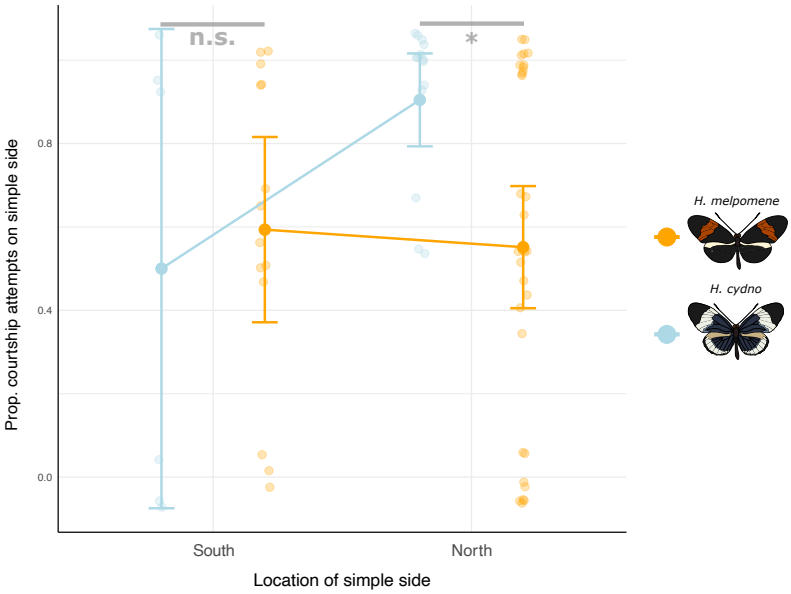


Figure 13 | The relative numbers of courtship attempts by *H. melpomene* (orange) and *H. cydno* (blue) did not significantly differ between the simple and complex sides. Each point represents data recorded for one individual during one trial.

Figure 14 | The relative numbers of courtship attempts by *H. melpomene* (orange) and *H. cydno* (blue) in the simple/complex sides significantly differed in one cage orientation, but not the other. Solid points indicate the mean simple/complex proportion for each species-orientation combination. Error bars represent 95% confidence intervals.

III.5 | Initial results do not indicate interspecific differences in navigation performance in a highly complex environment.

The pilot rotary obstacle experiment (19 unique butterflies: *H. cydno*: N = 9; *H. melpomene*: N = 10) showed that the traversal ability of the butterflies was not dramatically influenced by rotation speed, contrary to expectations. Variation in spinning speed from 3 to 18 RPM had no effect on crossing time (Anova: X^2 = 0.5160, df = 1, p=0.472). Additionally, there was no species effect, indicating that both species crossed the obstacle at the same speed (Anova: X^2 = 0.1014, df = 1, p=0.7502), and there was no statistical support for an interaction between species and speed (Anova: X^2 = 2.6219, df = 1, p=0.1054).

IV. Discussion

The evolution of visual acuity differences between closely related yet ecologically distinct species of *Heliconius* butterflies calls for disentanglement of the selection pressures driving visual evolution. Although it remains largely unexplored, this pattern is generally explained as parallel cases of local adaptation, where contrasting levels of vegetation density impose various selection pressures on sensory systems. Testing this hypothesis requires careful consideration of the ecological contexts in which distinct levels of visual acuity may drive fitness differences between species. Although this study represents an attempt at such characterization, the data I collected generally fails to highlight significant differences in the behavioural responses of *Heliconius cydno* and *Heliconius melpomene* to disparate levels of spatial complexity. This pattern held true across several ecological contexts.

Experienced levels of spatial complexity are likely the combined product of both environmental and behavioural patterns.

In the wild, I readily observed *H. melpomene* in disturbed areas characterized by a mosaic of secondary forest patches and deforested land. *H. cydno*, in contrast, was more abundant in closed-canopy forest, in the apparent absence of other *Heliconius* species. This is broadly consistent with previous observations from Panama (Estrada & Jiggins, 2002), which highlighted a progressive shift in *Heliconius* community makeup from closed-canopy forests to open terrain. Further, the natural habitats sampled for *H. cydno* and *H. melpomene* differed in canopy cover, but not in understorey conditions. This is an important result that seems to indicate that, while different forest types harbor distinct vegetation structures across their vertical amplitude, the physical blockage caused by vegetation may remain similar in the lower strata. In contrast, spatial complexity can be expected to decrease rapidly in less dense, secondary forests, moving away from the forest floor. This could explain the comparatively low canopy cover that characterizes *H. melpomene* localities. Importantly, it also raises the possibility that flight height may be a plastic modulator of spatial complexity in *Heliconius* habitats. This is not unlikely, since adaptation to local forest structure via flight height shifts has already been documented in other *Heliconius* species, albeit in the context of foraging (Dell'Aglio et al., 2022). Preliminary data show that *H. melpomene* and *H. cydno* also significantly differ in average flight height, but whether these differences are adaptive and relate to spatial complexity is a question that remains to be thoroughly addressed. More generally, this result implies that the flight height and visual systems may be closely linked. A close relationship between the two is already known from other insects, such as bees and fruit flies (Baird et al., 2006; Straw et al., 2010), but whether flight height can help maintain optimal

conditions for vision remains unclear. Flight behaviour is highly plastic, and might play an important role during habitat shifts, by avoiding mismatches between visual systems and the navigational requirements they satisfy. It is broadly accepted that plasticity can help bridge adaptive gaps during adaptation to a novel environment (Yeh & Price, 2004; Gross et al., 2010), and this may represent a novel example to be investigated in future work.

Disparate levels of visual acuity may not entail different levels of navigation performance.

Behavioural experiments showed that, comparing across environments, relative activity levels and navigation performance did not significantly differ between species. *H. melpomene* was significantly more active than its sister species in absolute terms, but it was not significantly more impacted than *H.* cydno when complexity increased. Additionally, both species were significantly more active when flying through a spatially simple environment. If open environments broadly facilitate high activity in *Heliconius* butterflies, it is possible that heritable differences in base activity evolved as habitat preferences diverged. If true, this may represent an important tradeoff in resource exploitation, whereby the cost of habitat exploration is kept stable through a balance between habitat complexity and travel distance. Controlling for fixed differences, however, this combined evidence does not support the existence of distinct reaction norms between species. If mismatches between visual acuity and local spatial complexity do not significantly impair navigation, navigational needs are unlikely to have driven visual evolution in the first place. Accordingly, recent morphometric dataset suggests that *H. melpomene* has a similar, but lower wing aspect ratio than *H. cydno* (Montejo-Kovacevich et al., 2019). This opposes the idea that *cydno* is the better navigator, since rounder wings are expected to positively affect maneuverability, an important trait in complex habitats (Chazot et al., 2016). Finally, the obstacle traversal capabilities of both species far exceeded reasonable expectations for natural levels of spatial complexity. In summary, though, there is a relative lack of evidence for the role of vegetation density as a major source of selection in the *melpomene/cydno* clade, even more so regarding divergent selection in visual systems.

Host plant search likely remains unaffected by local variation in spatial complexity.

H. melpomene and *H. cydno* did not show significantly different habitat preferences for oviposition, although a clear trend could be observed. *H. melpomene* laying predominantly in more open environments than those preferred by *H. cydno* would be expected, due to its lower visual acuity. Divergent preferences for oviposition environments would also be consistent with the observed distributions of these butterflies in the wild, and actively contribute to reproductive isolation by maintaining the spatial clustering of individuals at both the larval and adult stages (Nosil, 2012). Should

this trend be entirely spurious, however, an absence of distinct preferences may be interpreted in two ways. First, visual obstruction may not be limiting for host resource location in the first place, since *Heliconius* butterflies are known to also rely on olfaction to find suitable host plants (Thiele et al., 2016). Second, spatial segregation between species could simply involve divergence in host plant preferences. There is evidence for such divergence between the two species, where *H. melpomene* is likely more specialized (Merrill et al., 2013), and the distribution of the butterflies may thus mirror that of their preferred host plants. Should some *Passiflora* species depend on local spatial complexity for their establishment (e.g. due to local light conditions), patterns of distribution in host plants may drive habitat-species associations. This, however, would not explain divergence in visual systems.

Could the wing patterns of *H. cydno* and *H. melpomene* perform differently across different habitats?

The proportion of courtship attempts in simple and complex environments did not significantly differ between species. This may suggest that *H. melpomene* and *H. cydno* do not differ in their preferred mating environments. Alternatively, this may mean that variation in local spatial complexity has a similar impact on the mate search performance of *H. melpomene* and *H. cydno*. The effective range of sexual signals depends on both their ability to propagate through the environment and the sensory characteristics of its recipient. From a signal-centric point of view, local spatial complexity may not affect the range of *H. cydno* and *H. melpomene* warning patterns differently. Instead, range could depend on the sole effect of line-of-sight obstruction by vegetation, which should be comparable between these two similarly sized species. From an eye-centric perspective, variation in spatial complexity may challenge the vision of either species similarly, despite their different absolute levels of visual acuity. This is still to be taken with caution, since this specific test nearly reached statistical significance**.** In contrast, the fact that simple/complex courtship proportions were significantly affected by the cage orientation—species interaction could imply that signal effectiveness does depend on other external factors. Recent research (Hausmann et al., 2021) has highlighted significant differences in *Heliconius* mating signal efficacy across distinct light environments. In my experiment, artificial vine densities dramatically differed between the simple and complex sides of the experimental insectary, likely generating ample variation in local light conditions. An interpretation of the data could be that the processing of visual signals depends on their perceived brightness and is divergent between species. Caution should also be exercised here, however, since analyzing the effect of cage orientation required partitioning the dataset into subsets of unequal sizes. In fact, only 6 courtship attempts were recorded for *H. cydno* in the complex side was oriented northward, introducing significant uncertainty.

Assessing microhabitat differences in the wild likely demands new technologies.

Accurate characterization and understanding of wild habitats are a necessary first step in elucidating the ecological basis of sensory evolution. In the context of animal vision, photographic surveys are a powerful tool to assess habitat structure, but readily fail to integrate perceptive biases induced by visual systems. Modalities of information acquisition and processing can be extremely variable between taxa (Webster, 2015), and accurate visual models are essential to extract meaningful data from unprocessed images. In *Heliconius* butterflies, such models are still in their infancy (Dell'Aglio et al., 2018), but preliminary data suggest a dramatic decline in perceived detail as distance increases (Wright et al., 2023). Thus, while the photographs taken for this study should accurately reflect overall environment structure, they do not inform about perceived levels of spatial complexity. Instead, these likely depend on the lower-level organization of vegetation. Incorporating comprehensive depth information in future surveys would thus greatly enhance our ability to discriminate distinct perceptual environments, a more biologically relevant issue. Lidar technology, for example, has seen increasing use in recent years for habitat mapping (Hyde et al., 2005; Vierling et al., 2008; Guo et al., 2017) and may to be prove a powerful tool in assessing habitat microstructure. Likewise, because experienced levels of spatial complexity probably depend on flight height, future surveys should aim to integrate this characteristic into their protocols to reflect focal environments more accurately. Whether this is feasible in practice, however, is uncertain.

Deciphering the ecological basis of visual divergence in *Heliconius* butterflies requires extensive and targeted data collection.

Although common-garden trials generally failed to detect expected differences between *Heliconius cydno* and *Heliconius melpomene*, these experiments represent an important step in assessing the importance of visual acuity for various facets of *Heliconius* ecology. Indeed, examining ecological components in isolation is essential to identify the nature of the selection pressures acting on the visual systems of these butterflies. Accordingly, a recent model-based analysis (Dell'Aglio et al., 2018) disproved the long-running hypothesis that coevolution between a wing pigment and an opsin gene had been driven by predation pressures. While my work attempted to treat ecological contexts in isolation, future studies should focus on eliminating potential confounding factors. For example, allowing the butterflies to experience both treatments in quick succession, let alone freely within the same insectary, may have introduced noise via the averaging of local conditions. This effect could also be amplified by the generally small sizes of experimental insectaries, calling for careful consideration of cage dimensions when conducting behavioural trials. Similarly, while the rotary obstacle

experiment used traversal time to test obstacle avoidance, the results may reflect the general state of panic of the butterflies rather than their true flight "performance". Different metrics —*e.g.* number of collisions with obstacle, flight path deviation..— should perhaps be considered in the future to focus on flight quality or precision. A final point to consider is that of statistical power. Behavioural studies rely heavily on our ability to detect fine fluctuation between individual responses, but the overwhelming variability of behaviour makes this task difficult (Jennions & Møller, 2003). This is evidently true in *H. cydno* and *H*. *melpomene,* two incipient species that still share large aspects of their ecologies. On the one hand, the true effect sizes of their difference in visual acuity are expected to be small. On the other, large intraspecific diversity in both visual acuity (J. Borrero, D. Lozano, G. Rueda; unpublished data) and behavioural responses further challenges our ability to distinguish signal from noise. Promising trends in my data suggest, however, that future studies with larger sample sizes may identify distinct responses from both species, notably in the context of mate choice in variably complex environment. Importantly, the *Heliconius* genus comprises other species pairs with similar patterns of visual acuity and habitat use (*e.g. Heliconius himera* and *Heliconius erato cyrbia*, Wright et al., *unpublished data*). This represents an exciting opportunity to investigate repeated patterns of sensory adaptation at the species boundary and their ecological basis, calling for future work.

V. Acknowledgements

I would like to express my sincere gratitude to Geraldine Rueda and Daniela Lozano for their unwavering friendship, kindness and support throughout my stay in Colombia. I also thank them for a number of discussions that helped improve experimental designs. Many thanks to José Borrero and Richard Merrill for providing critical advice at various stages of this project, and for kindly reviewing an earlier version of this manuscript. Finally, I would like to extend my appreciation to Carolina Pardo Díaz for assisting me with important logistics and administrative processes during my time in Colombia, and to the whole team of the JCM research station for their warm welcome.

VI. References

Baird, E., Srinivasan, M. V., Zhang, S., Lamont, R., & Cowling, A. (2006). Visual Control of Flight Speed and Height in the Honeybee. In S. Nolfi, G. Baldassarre, R. Calabretta, J. C. T. Hallam, D. Marocco, J.-A. Meyer, O. Miglino, & D. Parisi (Eds.), *From Animals to Animats 9* (pp. 40–51). Springer Berlin Heidelberg.

Bates, D., Mächler, M., Bolker, B., & Walker, S. (2015). Fitting Linear Mixed-Effects Models Using lme4. *Journal of Statistical Software*, *67*(1), 1–48. https://doi.org/10.18637/jss.v067.i01

Beltrán, M., Jiggins, C. D., Bull, V., Linares, M., Mallet, J., McMillan, W. O., & Bermingham, E. (2002). Phylogenetic Discordance at the Species Boundary: Comparative Gene Genealogies Among Rapidly Radiating Heliconius Butterflies. *Molecular Biology and Evolution*, *19*(12), 2176–2190. https://doi.org/10.1093/oxfordjournals.molbev.a004042

Boughman, J. W. (2002). How sensory drive can promote speciation. *Trends in Ecology & Evolution*, *17*(12), 571–577. https://doi.org/10.1016/S0169-5347(02)02595-8

Brooks, M. E., Kristensen, K., Benthem, K. J. van, Magnusson, A., Berg, C. W., Nielsen, A., Skaug, H. J., Mächler, M., & Bolker, B. M. (2017). glmmTMB Balances Speed and Flexibility Among Packages for Zero-inflated Generalized Linear Mixed Modeling. *The R Journal*, *9*(2), 378–400. https://doi.org/10.32614/RJ-2017-066

Chazot, N., Panara, S., Zilbermann, N., Blandin, P., Le Poul, Y., Cornette, R., Elias, M., & Debat, V. (2016). Morpho morphometrics: Shared ancestry and selection drive the evolution of wing size and shape in Morpho butterflies. *Evolution*, *70*(1), 181–194. https://doi.org/10.1111/evo.12842

Crawley, M. J. (2002). *Review of Statistical computing: An introduction to data analysis using S-PLUS* (Vol. 42). John Wiley & Sons.

Cummings, M. E., & Endler, J. A. (2018). 25 Years of sensory drive: The evidence and its watery bias. *Current Zoology*, *64*(4), 471–484. https://doi.org/10.1093/cz/zoy043

Dell'Aglio, D. D., Mena, S., Mauxion, R., McMillan, W. O., & Montgomery, S. H. (2022). Divergence in Heliconius flight behaviour is associated with local adaptation to

different forest structures. *Journal of Animal Ecology*, *91*(4), 727–737. https://doi.org/10.1111/1365-2656.13675

Dell'Aglio, D. D., Troscianko, J., McMillan, W. O., Stevens, M., & Jiggins, C. D. (2018). The appearance of mimetic Heliconius butterflies to predators and conspecifics. *Evolution*, *72*(10), 2156–2166. https://doi.org/10.1111/evo.13583

Douma, J. C., & Weedon, J. T. (2019). Analysing continuous proportions in ecology and evolution: A practical introduction to beta and Dirichlet regression. *Methods in Ecology and Evolution*, *10*(9), 1412–1430. https://doi.org/10.1111/2041-210X.13234

Endler, J. A. (1992). Signals, Signal Conditions, and the Direction of Evolution. *The American Naturalist*, *139*, S125–S153.

Estrada, C., & Jiggins, C. D. (2002). Patterns of pollen feeding and habitat preference among Heliconius species. *Ecological Entomology*, *27*(4), 448–456. https://doi.org/10.1046/j.1365-2311.2002.00434.x

Fox, J., & Weisberg, S. (2019). *An R Companion to Applied Regression* (Third). Sage. https://socialsciences.mcmaster.ca/jfox/Books/Companion/

Gross, K., Pasinelli, G., & Kunc, H. P. (2010). Behavioral Plasticity Allows Short-Term Adjustment to a Novel Environment. *The American Naturalist*, *176*(4), 456–464. https://doi.org/10.1086/655428

Guo, Q., Su, Y., Hu, T., Zhao, X., Wu, F., Li, Y., Liu, J., Chen, L., Xu, G., Lin, G., Zheng, Y., Lin, Y., Mi, X., Fei, L., & Wang, X. (2017). An integrated UAV-borne lidar system for 3D habitat mapping in three forest ecosystems across China. *International Journal of Remote Sensing*, *38*(8–10), 2954–2972. https://doi.org/10.1080/01431161.2017.1285083

Halekoh, U., & Højsgaard, S. (2014). A Kenward-Roger Approximation and Parametric Bootstrap Methods for Tests in Linear Mixed Models – The R Package pbkrtest. *Journal of Statistical Software*, *59*(9), 1–32. https://doi.org/10.18637/jss.v059.i09

Hausmann, A. E., Kuo, C.-Y., Freire, M., Rueda-M, N., Linares, M., Pardo-Diaz, C., Salazar, C., & Merrill, R. M. (2021). Light environment influences mating behaviours during the early stages of divergence in tropical butterflies. *Proceedings of the Royal Society B: Biological Sciences*, *288*(1947). https://doi.org/10.1098/rspb.2021.0157

Hyde, P., Dubayah, R., Peterson, B., Blair, J. B., Hofton, M., Hunsaker, C., Knox, R., & Walker, W. (2005). Mapping forest structure for wildlife habitat analysis using waveform lidar: Validation of montane ecosystems. *Remote Sensing of Environment*, *96*(3), 427–437. https://doi.org/10.1016/j.rse.2005.03.005

Jennions, M. D., & Møller, A. P. (2003). A survey of the statistical power of research in behavioral ecology and animal behavior. *Behavioral Ecology*, *14*(3), 438–445. https://doi.org/10.1093/beheco/14.3.438

Maan, M. E., Hofker, K. D., van Alphen, J. J. M., & Seehausen, O. (2006). Sensory Drive in Cichlid Speciation. *The American Naturalist*, *167*(6), 947–954. https://doi.org/10.1086/503532

Maan, M. E., Seehausen, O., & Groothuis, T. G. G. (2017). Differential Survival between Visual Environments Supports a Role of Divergent Sensory Drive in Cichlid Fish Speciation. *The American Naturalist*, *189*(1), 78–85. https://doi.org/10.1086/689605

Mallet, J., McMillan, W. O., & Jiggins, C. (1998a). Mimicry and warning colour at the boundary between races and species. *Howard, D.J. and Berlocher, S.H. (Eds) Endless Forms: Species and Speciation*, 390–403.

Mallet, J., McMillan, W. O., & Jiggins, C. D. (1998b). Estimating The Mating Behavior Of A Pair Of Hybridizing *Heliconius* Species In The Wild. *Evolution*, *52*(2), 503–510. https://doi.org/10.1111/j.1558-5646.1998.tb01649.x

Merrill, R. M., Naisbit, R. E., Mallet, J., & Jiggins, C. D. (2013). Ecological and genetic factors influencing the transition between host-use strategies in sympatric Heliconius butterflies. *Journal of Evolutionary Biology*, *26*(9), 1959–1967. https://doi.org/10.1111/jeb.12194

Montejo-Kovacevich, G., Smith, J. E., Meier, J. I., Bacquet, C. N., Whiltshire-Romero, E., Nadeau, N. J., & Jiggins, C. D. (2019). Altitude and life-history shape the evolution of Heliconius wings. *Evolution*, *73*(12), 2436–2450. https://doi.org/10.1111/evo.13865

Montgomery, S. H., & Merrill, R. (2017). Divergence in brain composition during the early stages of ecological specialization in Heliconius butterflies. *Journal of Evolutionary Biology*, *30*(3), 571–582. https://doi.org/10.1111/jeb.13027

Montgomery, S. H., Rossi, M., McMillan, W. O., & Merrill, R. M. (2021). Neural divergence and hybrid disruption between ecologically isolated *Heliconius* butterflies.

Proceedings of the National Academy of Sciences, *118*(6), e2015102118. https://doi.org/10.1073/pnas.2015102118

Müller, F. (1879). Ituna and Thyridia; a remarkable case of mimicry in butterflies. *Transactions of the Entomological Society of London*, *xx*, xxix.

Nosil, P. (2012). *Ecological speciation*. Oxford University Press.

R Core Team. (2023). *R: A Language and Environment for Statistical Computing*. R Foundation for Statistical Computing. https://www.R-project.org/

Rice, W. R. (1987). Speciation via habitat specialization: The evolution of reproductive isolation as a correlated character. *Evolutionary Ecology*, *1*(4), 301–314. https://doi.org/10.1007/BF02071555

Schneider, C. A., Rasband, W. S., & Eliceiri, K. W. (2012). NIH Image to ImageJ: 25 years of image analysis. *Nature Methods*, *9*(7), 671–675. https://doi.org/10.1038/nmeth.2089

Seehausen, O., Terai, Y., Magalhaes, I. S., Carleton, K. L., Mrosso, H. D. J., Miyagi, R., van der Sluijs, I., Schneider, M. V., Maan, M. E., Tachida, H., Imai, H., & Okada, N. (2008). Speciation through sensory drive in cichlid fish. *Nature*, *455*(7213), 620–626. https://doi.org/10.1038/nature07285

Seymoure, B. M., Mcmillan, W. O., & Rutowski, R. (2015). Peripheral eye dimensions in Longwing (Heliconius) butterflies vary with body size and sex but not light environment nor mimicry ring. *The Journal of Research on the Lepidoptera*, *48*, 83–92.

Straw, A. D., Lee, S., & Dickinson, M. H. (2010). Visual control of altitude in flying Drosophila. *Current Biology*, *20*(17), 1550–1556.

Thiele, S. C., Rodrigues, D., & Moreira, G. R. P. (2016). Oviposition in Heliconius erato (Lepidoptera, Nymphalidae): How Essential Is Drumming Behavior for Host-Plant Selection? *Journal of Insect Behavior*, *29*(3), 283–300. https://doi.org/10.1007/s10905-016-9559-z

Vierling, K. T., Vierling, L. A., Gould, W. A., Martinuzzi, S., & Clawges, R. M. (2008). Lidar: Shedding new light on habitat characterization and modeling. *Frontiers in Ecology and the Environment*, *6*(2), 90–98. https://doi.org/10.1890/070001

Webster, M. A. (2015). Visual Adaptation. *Annual Review of Vision Science*, *1*(1), 547–567. https://doi.org/10.1146/annurev-vision-082114-035509

Wickham, H. (2011). Ggplot2. *WIREs Computational Statistics*, *3*(2), 180–185. https://doi.org/10.1002/wics.147

Wright, D. S., Manel, A. N., Guachamin-Rosero, M., Chamba-Vaca, P., Bacquet, C. N., & Merrill, R. M. (2023). Quantifying visual acuity in Heliconius butterflies. *Biology Letters*, *19*(12), 20230476. https://doi.org/10.1098/rsbl.2023.0476

Yeh, P. J., & Price, T. D. (2004). Adaptive Phenotypic Plasticity and the Successful Colonization of a Novel Environment. *The American Naturalist*, *164*(4), 531–542. https://doi.org/10.1086/423825

VII. Appendices

Table S1 | Wild individual data.

Species	Number	ID	Sex	Morph	Pollen	Time	Date	Body length	Flight height	Description	Latitude	Longitude	Locality
C	29	C029	m	yellow	high	9:56	1.01	32mm	310cm		4.9476632	-74.36998	PAR
C	30	C030	m	white	none	11:37	10.01	31mm	260cm		4.9480598	-74.370159	PAR
M	8	M008	f	typical	low	12:48	10.01	25mm	40cm		4.9479454	-74.370271	PAR
C	26	C026	f	white	none	9:21	10.01	28mm	150cm		4.948692	-74.37021	PAR
M	6	M006	m	typical	none	9:31	10.01	28mm	140cm		4.94846	-74.370259	PAR
M	7	M007	m	typical	none	9:36	10.01	29mm	120cm		4.9480542	-74.3702	PAR
C	27	C027	m	yellow	low	9:37	10.01	30mm	120cm	Same spot as m007	4.9480548	-74.370182	PAR
C	28	C028	m	white	low	9:40	10.01	28mm	70cm		4.9481176	-74.370171	PAR
C	11	C011	m	white	none	11:20	11.1	28mm	500cm		4.9571332	-74.379798	CCF
C	10	C010	m	white	none	11:55	11.1	30mm	140cm		4.9555203	-74.379299	CCF
C	12	C012	f	white	none	11:45	12.1	29mm	20cm		4.9572394	-74.380209	CCF
C	13	C013	m	white	none	12:13	12.1	29mm	160cm		4.9572543	-74.380099	CCF
C	31	C031	m	yellow	none	10:58	14.01	28mm	110cm		4.9649097	-74.383766	RF
M	9	M009	m	typical	some	11:20	14.01	24mm	80cm		4.9649178	-74.38379	RF
C	32	C032	m	white	some	11:23	14.01	29mm	100cm		4.9648897	-74.383786	RF
C	33	C033	m	yellow	none	11:30	14.01	29mm	220cm	Same as m002	4.9647587	-74.383731	RF
C	34	C034	m	white	none	11:32	14.01	30mm	50cm	Same as M011	4.9647464	-74.383704	RF
M	10	M010	f	typical	none	11:50	14.01	29mm	100cm		4.9649208	-74.383813	RF
M	11	M011	m	typical	none	11:58	14.01	26mm	170cm		4.9647423	-74.38373	RF
C	14	C014	f	white	none	12:20	17.1	29mm	30cm	RH21 17.10 13:15 19.10 17.40	4.9555872	-74.379029	CCF
C	15	C015	f	white	low	12:23	17.1	28mm	250cm		4.9555744	-74.378938	CCF
C	16	C016	m	white	none	12:56	17.1	29mm	160cm		4.9555158	-74.378613	CCF
C	17	C017	m	white	none	13:13	17.1	29mm	80cm		4.9553544	-74.379988	CCF
C	18	C018	f	yellow	none	13:13	17.1	28mm	80cm		4.9552773	-74.380114	CCF
C	19	C019	m	white	none	17:15	19.1	NA	500cm		4.9572845	-74.380305	CCF
C	1	C001	m	white	NA	16:25	25.09	NA	NA		4.955398	-74.378113	CCF
C	2	C002	m	white	NA	NA	25.09	NA	80cm		4.955573	-74.378624	CCF
C	3	C003	m	yellow	NA	16:30	28.09	NA	90cm	RH21 11.10 13h 12.10 12h41	4.9554921	-74.378978	CCF
C	20	C020	f	yellow	none	11:55	28.1	29mm	280cm		4.9573591	-74.380057	CCF
C	22	C022	f	white	low	12:42	29.11	30mm	50cm		4.9555892	-74.379274	CCF
C	23	C023	m	white	none	12:48	29.11	31mm	200cm		4.9553162	-74.379608	CCF
M	1	M001	f	typical	high	10:43	3.1	23mm	20cm		4.9627413	-74.380235	RF

M	2	M002	m	typical	low	11:20	3.1	28mm	40cm		4.9647782	-74.383718	RF
M	3	M003	f	typical	low	11:45	3.1	22mm	40cm		4.9645857	-74.383862	RF
M	4	M004	f	typical	high	11:52	3.1	23mm	45cm		4.9645339	-74.383913	RF
M	5	M005	m	typical	none	12:05	3.1	25mm	65cm		4.9646993	-74.383848	RF
C	24	C024	f	white	none	11:53	3.12	28mm	130cm		4.9553477	-74.377745	CCF
C	25	C025	m	white	none	11:57	3.12	25mm	110cm		4.9553645	-74.377665	CCF
C	4	C004	f	white	NA	15:50	30.09	NA	110cm		4.9553454	-74.380038	CCF
C	5	C005	m	white	NA	16:05	30.09	NA	125cm		4.9557316	-74.379109	CCF
C	6	C006	f	white	NA	16:15	30.09	NA	30cm		4.9556369	-74.378877	CCF
C	7	C007	m	white	NA	16:50	30.09	NA	0cm		4.9555344	-74.378998	CCF
C	8	C008	f	white	none	12:30	5.1	NA	250cm		4.9556672	-74.379791	CCF
C	9	C009	f	white	none	12:00	7.1	28mm	260cm		4.9560296	-74.380299	CCF
C	21	C021	F	white	none	11:26	9.11	26mm	175cm		4.9554937	-74.380171	CCF

Table S2| Spatial complexity from photographic samples.

Species	Sample	Photograph	Obstruction (%)	Type	Locality
Cydno	C001	C001_1	52,6	Understorey	CCF
Cydno	C001	C001_2	22,9	Understorey	CCF
Cydno	C001	C001_3	23,9	Understorey	CCF
Cydno	C001	C001_4	25,6	Understorey	CCF
Cydno	C001	C001_5	97,2	Canopy	CCF
Cydno	C002	C002_1	33,2	Understorey	CCF
Cydno	C002	C002_2	54,5	Understorey	CCF
Cydno	C002	C002_3	60,5	Understorey	CCF
Cydno	C002	C002_4	50	Understorey	CCF
Cydno	C002	C002_5	98,4	Canopy	CCF
Cydno	C003	C003_1	26,2	Understorey	CCF
Cydno	C003	C003_2	29,7	Understorey	CCF
Cydno	C003	C003_3	34	Understorey	CCF
Cydno	C003	C003_4	41,7	Understorey	CCF
Cydno	C003	C003_5	93,9	Canopy	CCF
Cydno	C008	C008_1	40,7	Understorey	CCF
Cydno	C008	C008_2	17,1	Understorey	CCF
Cydno	C008	C008_3	37,9	Understorey	CCF
Cydno	C008	C008_4	55,7	Understorey	CCF
Cydno	C008	C008_5	92	Canopy	CCF
Cydno	C009	C009_1	45,7	Understorey	CCF
Cydno	C009	C009_2	70,2	Understorey	CCF
Cydno	C009	C009_3	60,5	Understorey	CCF
Cydno	C009	C009_4	40,9	Understorey	CCF
Cydno	C009	C009_5	87,7	Canopy	CCF
Cydno	C011	C011_1	29,7	Understorey	CCF
Cydno	C011	C011_2	61,4	Understorey	CCF
Cydno	C011	C011_3	18,7	Understorey	CCF
Cydno	C011	C011_4	28,6	Understorey	CCF
Cydno	C011	C011_5	84,8	Canopy	CCF
Cydno	C012	C012_1	15	Understorey	CCF
Cydno	C012	C012_2	31,08	Understorey	CCF
Cydno	C012	C012_3	49,9	Understorey	CCF
Cydno	C012	C012_4	43,9	Understorey	CCF
Cydno	C012	C012_5	91,6	Canopy	CCF
Cydno	C014	C014_1	64,6	Understorey	CCF
Cydno	C014	C014_2	14,6	Understorey	CCF
Cydno	C014	C014_3	32,5	Understorey	CCF
Cydno	C014	C014_4	29,1	Understorey	CCF
Cydno	C014	C014_5	92,2	Canopy	CCF
Cydno	C027	C027_1	31,5	Understorey	PAR
Cydno	C027	C027_2	22,7	Understorey	PAR
Cydno	C027	C027_3	13,9	Understorey	PAR
Cydno	C027	C027_4	43,29	Understorey	PAR

Cydno	C027	C027_5	85,6	Canopy	PAR
Cydno	C031	C031_1	8,5	Understorey	RF
Cydno	C031	C031_2	67,5	Understorey	RF
Cydno	C031	C031_3	8,5	Understorey	RF
Cydno	C031	C031_4	11	Understorey	RF
Cydno	C031	C031_5	0	Canopy	RF
Cydno	C033	C033_1	5,4	Understorey	RF
Cydno	C033	C033_2	43,4	Understorey	RF
Cydno	C033	C033_3	7,5	Understorey	RF
Cydno	C033	C033_4	46,2	Understorey	RF
Cydno	C033	C033_5	NA	Canopy	RF
Melpomene	M002	M002_1	42,6	Understorey	RF
Melpomene	M002	M002_2	30,1	Understorey	RF
Melpomene	M002	M002_3	38,3	Understorey	RF
Melpomene	M002	M002_4	40,6	Understorey	RF
Melpomene	M002	M002_5	46,7	Canopy	RF
Melpomene	M003	M003_1	21,4	Understorey	RF
Melpomene	M003	M003_2	45,4	Understorey	RF
Melpomene	M003	M003_3	22,2	Understorey	RF
Melpomene	M003	M003_4	49,3	Understorey	RF
Melpomene	M003	M003_5	87,2	Canopy	RF
Melpomene	M005	M005_1	47,1	Understorey	RF
Melpomene	M005	M005_2	42,7	Understorey	RF
Melpomene	M005	M005_3	36,6	Understorey	RF
Melpomene	M005	M005_4	48,8	Understorey	RF
Melpomene	M005	M005_5	59,7	Canopy	RF
Melpomene	M006	M006_1	17,8	Understorey	PAR
Melpomene	M006	M006_2	17,8	Understorey	PAR
Melpomene	M006	M006_3	17,8	Understorey	PAR
Melpomene	M006	M006_4	17,8	Understorey	PAR
Melpomene	M006	M006_5	40	Canopy	PAR
Melpomene	M007	M007_1	31,5	Understorey	PAR
Melpomene	M007	M007_2	22,7	Understorey	PAR
Melpomene	M007	M007_3	13,9	Understorey	PAR
Melpomene	M007	M007_4	43,29	Understorey	PAR
Melpomene	M007	M007_5	85,6	Canopy	PAR
Melpomene	M008	M008_1	40,5	Understorey	PAR
Melpomene	M008	M008_2	4,8	Understorey	PAR
Melpomene	M008	M008_3	8,6	Understorey	PAR
Melpomene	M008	M008_4	36,8	Understorey	PAR
Melpomene	M008	M008_5	52,9	Canopy	PAR
Melpomene	M009	M009_1	8,5	Understorey	RF
Melpomene	M009	M009_2	67,5	Understorey	RF
Melpomene	M009	M009_3	8,5	Understorey	RF
Melpomene	M009	M009_4	11	Understorey	RF
Melpomene	M009	M009_5	0	Canopy	RF
Melpomene	M011	M011_1	5,4	Understorey	RF
Melpomene	M011	M011_2	43,4	Understorey	RF
Melpomene	M011	M011_3	7,5	Understorey	RF
Melpomene	M011	M011_4	46,2	Understorey	RF
Melpomene	M011	M011_5	NA	Canopy	RF

Table S3| Data from the exploratory activity experiment.

Date	GroupID	Male	Species	Treatment	Score	Weather
16_09_2023	1	B23_498	Cydno	Simple	15	Cloudy
16_09_2023	1	B23_533	Melpomene	Simple	40	Cloudy
16_09_2023	1	B23_979	Cydno	Complex	26	Cloudy
16_09_2023	1	B23_708	Melpomene	Complex	6	Cloudy

16_09_2023	1	B23_979	Cydno	Simple	21	Cloudy
16_09_2023	1	B23_708	Melpomene	Simple	4	Cloudy
16_09_2023	1	B23_498	Cydno	Complex	6	Cloudy
16_09_2023	1	B23_533	Melpomene	Complex	5	Cloudy
16_09_2023	2	B23_516	Cydno	Simple	20	Sunny
16_09_2023	2	B23_969	Melpomene	Simple	28	Sunny
16_09_2023	2	B23_401	Cydno	Complex	19	Sunny
16_09_2023	2	B23_790	Melpomene	Complex	52	Sunny
16_09_2023	2	B23_401	Cydno	Simple	30	Sunny
16_09_2023	2	B23_790	Melpomene	Simple	37	Sunny
16_09_2023	2	B23_516	Cydno	Complex	5	Sunny
16_09_2023	2	B23_969	Melpomene	Complex	20	Sunny
17_09_2023	3	B23_922	Cydno	Simple	42	Overcast
17_09_2023	3	B23_116	Melpomene	Simple	14	Overcast
17_09_2023	3	B23_456	Cydno	Complex	4	Overcast
17_09_2023	3	B23_177	Melpomene	Complex	31	Overcast
17_09_2023	3	B23_456	Cydno	Simple	3	Cloudy
17_09_2023	3	B23_177	Melpomene	Simple	14	Cloudy
17_09_2023	3	B23_922	Cydno	Complex	11	Cloudy
17_09_2023	3	B23_116	Melpomene	Complex	13	Cloudy
17_09_2023	4	B23_471	Cydno	Simple	36	Overcast
17_09_2023	4	B23_772	Melpomene	Simple	18	Overcast
17_09_2023	4	B23_498	Cydno	Complex	8	Overcast
17_09_2023	4	B23_686	Melpomene	Complex	0	Overcast
17_09_2023	4	B23_498	Cydno	Simple	0	Overcast
17_09_2023	4	B23_686	Melpomene	Simple	10	Overcast
17_09_2023	4	B23_471	Cydno	Complex	12	Overcast
17_09_2023	4	B23_772	Melpomene	Complex	2	Overcast
18_09_2023	5	B23_922	Cydno	Simple	26	Cloudy
18_09_2023	5	B23_944	Melpomene	Simple	28	Cloudy
18_09_2023	5	B23_979	Cydno	Complex	44	Cloudy
18_09_2023	5	B23_969	Melpomene	Complex	0	Cloudy
18_09_2023	5	B23_979	Cydno	Simple	1	Cloudy
18_09_2023	5	B23_969	Melpomene	Simple	5	Cloudy
18_09_2023	5	B23_922	Cydno	Complex	3	Cloudy
18_09_2023	5	B23_944	Melpomene	Complex	9	Cloudy
18_09_2023	6	B23_401	Cydno	Simple	11	Cloudy
18_09_2023	6	B23_436	Melpomene	Simple	43	Cloudy
18_09_2023	6	B23_498	Cydno	Complex	3	Cloudy
18_09_2023	6	B23_497	Melpomene	Complex	8	Cloudy
18_09_2023	6	B23_498	Cydno	Simple	0	Cloudy
18_09_2023	6	B23_497	Melpomene	Simple	32	Cloudy
18_09_2023	6	B23_401	Cydno	Complex	20	Cloudy
18_09_2023	6	B23_436	Melpomene	Complex	12	Cloudy
18_09_2023	7	B23_779	Cydno	Simple	13	Cloudy
18_09_2023	7	B23_874	Melpomene	Simple	58	Cloudy
18_09_2023	7	B23_836	Cydno	Complex	10	Cloudy
18_09_2023	7	B23_889	Melpomene	Complex	11	Cloudy
18_09_2023	7	B23_836	Cydno	Simple	4	Cloudy
18_09_2023	7	B23_889	Melpomene	Simple	3	Cloudy
18_09_2023	7	B23_779	Cydno	Complex	0	Cloudy
18_09_2023	7	B23_874	Melpomene	Complex	12	Cloudy
19_09_2023	8	B23_778	Cydno	Simple	26	Cloudy
19_09_2023	8	B23_823	Melpomene	Simple	63	Cloudy
19_09_2023	8	B23_638	Cydno	Complex	70	Cloudy
19_09_2023	8	B23_889	Melpomene	Complex	70	Cloudy
19_09_2023	8	B23_638	Cydno	Simple	24	Overcast
19_09_2023	8	B23_889	Melpomene	Simple	10	Overcast
19_09_2023	8	B23_778	Cydno	Complex	3	Overcast
19_09_2023	8	B23_823	Melpomene	Complex	25	Overcast

19_09_2023	9	B23_661	Cydno	Simple	34	Overcast
19_09_2023	9	B23_961	Melpomene	Simple	32	Overcast
19_09_2023	9	B23_578	Cydno	Complex	33	Overcast
19_09_2023	9	B23_942	Melpomene	Complex	13	Overcast
19_09_2023	9	B23_578	Cydno	Simple	16	Cloudy
19_09_2023	9	B23_942	Melpomene	Simple	5	Cloudy
19_09_2023	9	B23_661	Cydno	Complex	10	Cloudy
19_09_2023	9	B23_961	Melpomene	Complex	9	Cloudy
21_09_2023	10	B23_777	Cydno	Simple	0	Sunny
21_09_2023	10	B23_997	Melpomene	Simple	18	Sunny
21_09_2023	10	B23_810	Cydno	Complex	29	Sunny
21_09_2023	10	B23_992	Melpomene	Complex	112	Sunny
21_09_2023	10	B23_810	Cydno	Simple	13	Cloudy
21_09_2023	10	B23_992	Melpomene	Simple	65	Cloudy
21_09_2023	10	B23_777	Cydno	Complex	0	Cloudy
21_09_2023	10	B23_997	Melpomene	Complex	2	Cloudy
21_09_2023	11	B23_578	Cydno	Simple	5	Cloudy
21_09_2023	11	B23_943	Melpomene	Simple	22	Cloudy
21_09_2023	11	B23_962	Cydno	Complex	0	Cloudy
21_09_2023	11	B23_895	Melpomene	Complex	24	Cloudy
21_09_2023	11	B23_962	Cydno	Simple	0	Cloudy
21_09_2023	11	B23_895	Melpomene	Simple	3	Cloudy
21_09_2023	11	B23_578	Cydno	Complex	2	Cloudy
21_09_2023	11	B23_943	Melpomene	Complex	1	Cloudy
22_09_2023	12	B23_441	Cydno	Simple	11	Cloudy
22_09_2023	12	B23_887	Melpomene	Simple	23	Cloudy
22_09_2023	12	B23_813	Cydno	Complex	6	Cloudy
22_09_2023	12	B23_720	Melpomene	Complex	2	Cloudy
22_09_2023	12	B23_813	Cydno	Simple	12	Cloudy
22_09_2023	12	B23_720	Melpomene	Simple	10	Cloudy
22_09_2023	12	B23_441	Cydno	Complex	3	Cloudy
22_09_2023	12	B23_887	Melpomene	Complex	61	Cloudy
26_09_2023	13	B23_456	Cydno	Simple	0	Overcast
26_09_2023	13	B23_944	Melpomene	Simple	0	Overcast
26_09_2023	13	B23_401	Cydno	Complex	43	Overcast
26_09_2023	13	B23_686	Melpomene	Complex	0	Overcast
26_09_2023	13	B23_401	Cydno	Simple	33	Cloudy
26_09_2023	13	B23_686	Melpomene	Simple	26	Cloudy
26_09_2023	13	B23_456	Cydno	Complex	0	Cloudy
26_09_2023	13	B23_944	Melpomene	Complex	0	Cloudy
26_09_2023	14	B23_471	Cydno	Simple	79	Cloudy
26_09_2023	14	B23_772	Melpomene	Simple	5	Cloudy
26_09_2023	14	B23_922	Cydno	Complex	4	Cloudy
26_09_2023	14	B23_177	Melpomene	Complex	0	Cloudy
26_09_2023	14	B23_922	Cydno	Simple	7	Cloudy
26_09_2023	14	B23_177	Melpomene	Simple	71	Cloudy
26_09_2023	14	B23_471	Cydno	Complex	2	Cloudy
26_09_2023	14	B23_772	Melpomene	Complex	0	Cloudy
27_09_2023	15	B23_779	Cydno	Simple	32	Sunny
27_09_2023	15	B23_961	Melpomene	Simple	22	Sunny
27_09_2023	15	B23_580	Cydno	Complex	4	Sunny
27_09_2023	15	B23_874	Melpomene	Complex	125	Sunny
27_09_2023	15	B23_580	Cydno	Simple	0	Overcast
27_09_2023	15	B23_874	Melpomene	Simple	2	Overcast
27_09_2023	15	B23_779	Cydno	Complex	4	Overcast
27_09_2023	15	B23_961	Melpomene	Complex	6	Overcast
29_09_2023	16	B23_578	Cydno	Simple	15	Sunny
29_09_2023	16	B23_943	Melpomene	Simple	45	Sunny
29_09_2023	16	B23_112	Cydno	Complex	10	Sunny
29_09_2023	16	B23_932	Melpomene	Complex	98	Sunny

29_09_2023	16	B23_112	Cydno	Simple	0	Cloudy
29_09_2023	16	B23_932	Melpomene	Simple	41	Cloudy
29_09_2023	16	B23_578	Cydno	Complex	3	Cloudy
29_09_2023	16	B23_943	Melpomene	Complex	2	Cloudy
29_09_2023	17	B23_836	Cydno	Simple	6	Sunny
29_09_2023	17	B23_873	Melpomene	Simple	50	Sunny
29_09_2023	17	B23_839	Cydno	Complex	19	Sunny
29_09_2023	17	B23_993	Melpomene	Complex	1	Sunny
29_03_2023	17	B23_839	Cydno	Simple	19	Cloudy
29_03_2023	17	B23_993	Melpomene	Simple	0	Cloudy
29_03_2023	17	B23_836	Cydno	Complex	2	Cloudy
29_03_2023	17	B23_873	Melpomene	Complex	15	Cloudy
30_09_2023	18	B23_661	Cydno	Simple	39	Sunny
30_09_2023	18	B23_895	Melpomene	Simple	21	Sunny
30_09_2023	18	B23_810	Cydno	Complex	1	Sunny
30_09_2023	18	B23_903	Melpomene	Complex	35	Sunny
30_09_2023	18	B23_810	Cydno	Simple	2	Sunny
30_09_2023	18	B23_903	Melpomene	Simple	5	Sunny
30_09_2023	18	B23_661	Cydno	Complex	0	Sunny
30_09_2023	18	B23_895	Melpomene	Complex	20	Sunny
30_09_2023	19	B23_710	Cydno	Simple	32	Sunny
30_09_2023	19	B23_978	Melpomene	Simple	128	Sunny
30_09_2023	19	B23_2	Cydno	Complex	9	Sunny
30_09_2023	19	B23_823	Melpomene	Complex	26	Sunny
30_09_2023	19	B23_2	Cydno	Simple	0	Sunny
30_09_2023	19	B23_823	Melpomene	Simple	36	Sunny
30_09_2023	19	B23_710	Cydno	Complex	25	Sunny
30_09_2023	19	B23_978	Melpomene	Complex	52	Sunny
30_09_2023	20	B23_778	Cydno	Simple	5	Sunny
30_09_2023	20	B23_995	Melpomene	Simple	22	Sunny
30_09_2023	20	B23_962	Cydno	Complex	3	Sunny
30_09_2023	20	B23_975	Melpomene	Complex	30	Sunny
30_09_2023	20	B23_962	Cydno	Simple	4	Sunny
30_09_2023	20	B23_975	Melpomene	Simple	77	Sunny
30_09_2023	20	B23_778	Cydno	Complex	4	Sunny
30_09_2023	20	B23_995	Melpomene	Complex	14	Sunny
2_10_2023	21	B23_498	Cydno	Simple	12	Sunny
2_10_2023	21	B23_708	Melpomene	Simple	46	Sunny
2_10_2023	21	B23_777	Cydno	Complex	11	Sunny
2_10_2023	21	B23_944	Melpomene	Complex	39	Sunny
2_10_2023	21	B23_777	Cydno	Simple	2	Cloudy
2_10_2023	21	B23_944	Melpomene	Simple	8	Cloudy
2_10_2023	21	B23_498	Cydno	Complex	1	Cloudy
2_10_2023	21	B23_708	Melpomene	Complex	0	Cloudy
2_10_2023	22	B23_2	Cydno	Simple	17	Cloudy
2_10_2023	22	B23_894	Melpomene	Simple	5	Cloudy
2_10_2023	22	B23_638	Cydno	Complex	0	Cloudy
2_10_2023	22	B23_873	Melpomene	Complex	14	Cloudy
2_10_2023	22	B23_638	Cydno	Simple	0	Overcast
2_10_2023	22	B23_873	Melpomene	Simple	0	Overcast
2_10_2023	22	B23_2	Cydno	Complex	1	Overcast
2_10_2023	22	B23_894	Melpomene	Complex	0	Overcast

Table S4| Data from the oviposition experiment.

Female	Species	Origin	Location	Date start	Date end	Totaleggs_S	Totaleggs_C	Vine configuration
B23_657	C	NA	56	09_10_2023	14_10_2023	2	5	low_density
C23_149	M	NA	43	17_10_2023	19_10_2023	0	0	low_density
C23_119	C	NA	56	17_10_2023	19_10_2023	1	8	low_density

C23_54	M	NA	56	20_10_2023	22_10_2023	1	9	low_density
C23_78	C	NA	43	20_10_2023	22_10_2023	0	0	low_density
C23_217	C	NA	43	24_10_2023	26_10_2023	0	0	low_density
B23_965	M	NA	56	24_10_2023	26_10_2023	6	7	low_density
C23_237	M	18B	43	27_10_2023	29_10_2023	1	9	low_density
C23_084	C	11A	56	27_10_2023	29_10_2023	4	17	low_density
C23_259	C	13A	43	30_10_2023	01_11_2023	1	0	low_density
C23_239	M	19B	56	30_10_2023	01_11_2023	4	1	low_density
C23_271	C	11A	56	02_11_2023	04_11_2023	12	2	low_density
B23_967	M	13B	43	02_11_2023	04_11_2023	4	0	low_density
C23_142	M	13B	56	05_11_2023	08_11_2023	3	6	low_density
C23_178	C	13A	43	05_11_2023	08_11_2023	3	2	low_density
C23_427	M	13B	43	08_11_2023	10_11_2023	4	2	low_density
C23_244	C	13A	56	08_11_2023	10_11_2023	0	1	low_density
C23_335	C	13A	43	11_11_2023	13_11_2023	3	3	low_density
C23_034	M	13B	56	11_11_2023	13_11_2023			low_density
C23_427	M	13B	43	23_11_2023	27_11_2023	16	9	high_density
C23_398	C	13A	56	23_11_2023	27_11_2023	2	8	high_density
C23_537	C	13A	43	27_11_2023	29_11_2023	0	0	high_density
C23_328	M	18B	56	27_11_2023	29_11_2023	7	2	high_density
C23_054	M	19B	43	29_11_2023	01_12_2023	0	0	high_density
C23_457	C	11A	56	29_11_2023	02_12_2023	5	8	high_density
C23_244	C	13A	56	04_12_2023	06_12_2023	4	0	high_density
C23_371	M	13B	43	04_12_2023	06_12_2023	0	0	high_density
C23_569	C	11A	43	08_12_2023	10_12_2023	2	3	high_density
C23_439	M	18B	56	08_12_2023	10_12_2023	0	0	high_density
C23_442	M	19B	43	13_12_2023	15_12_2023	3	0	high_density
C23_579	C	11A	56	13_12_2023	15_12_2023	3	4	high_density
C23_442	M	19B	56	14_12_2023	16_12_2023	5	1	high_density
C23_569	C	NA	43	14_12_2023	16_12_2023	4	2	high_density
C23_237	M	NA	43	17_12_2023	19_12_2023	0	1	high_density
C23_569	C	NA	56	17_12_2023	19_12_2023	1	3	high_density
C23_573	M	NA	56	20_12_2023	22_12_2023	4	2	high_density
C23_569	C	11A	43	20_12_2023	22_12_2023	4	1	high_density
C23_731	M	19B	43	31_12_2023	03_01_2024	2	4	high_density
C23_781	C	11A	56	31_12_2023	03_01_2024	0	0	high_density
C23_780	C	11A	43	04_01_2024	06_01_2024	0	0	high_density
C23_793	M	18B	56	04_01_2024	06_01_2024	1	0	high_density
C23_869	C	11A	43	07_01_2024	09_01_2024	0	0	high_density
C23_680	M	13B	56	07_01_2024	09_01_2024	4	7	high_density
C23_781	C	11A	56	10_01_2024	12_01_2024	10	5	high_density
C23_735	M	13B	43	10_01_2024	12_01_2024	7	3	high_density
C23_572	M	18B	56	13_01_2024	15_01_2024	4	8	high_density
C23_945	C	11A	43	13_01_2024	15_01_2024	0	0	high_density
C23_515	Cy	20A	56	16_01_2024	18_01_2024	1	5	high_density
C23_922	M	13B	43	16_01_2024	18_01_2024	7	6	high_density
C23_945	C	11A	43	19_01_2024	21_01_2024	2	0	high_density
C23_951	M	13B	56	19_01_2024	21_01_2024	1	6	high_density
C23_735	M	13B	43	23_01_2024	25_01_2024	1	1	high_density
C23_768	Cy	20A	56	23_01_2024	25_01_2024	5	11	high_density

Table S5| Data from the mate choice experiment.

Date	Trial	Complex side	Weather	ID	Species	Count S	Count C	Count S*	Count C*	Total (simple)	Total (complex)	Total	Latency (simple)	Latency (complex)
08_11_2023	1	South	Overcast	C23_193	cydno	2	0	0	0	2	0	2	9	29
08_11_2023	1	South	Overcast	C23_370	melpomene	0	0	0	0	0	0	0	29	29
08_11_2023	2	South	Overcast	C23_261	cydno	0	0	0	0	0	0	0	29	29
08_11_2023	2	South	Overcast	C23_349	melpomene	0	0	0	0	0	0	0	29	29
08_11_2023	3	South	Overcast	C23_243	cydno	0	0	0	0	0	0	0	29	29
08_11_2023	3	South	Overcast	C23_436	melpomene	0	0	0	0	0	0	0	29	29
10_11_2023	1	South	Cloudy	C23_401	cydno	0	0	3	2	3	2	5	29	29
10_11_2023	1	South	Cloudy	B23_874	melpomene	2	3	0	0	2	3	5	22	0
10_11_2023	2	South	Cloudy	B23_922	cydno	0	0	2	0	2	0	2	29	29
10_11_2023	2	South	Cloudy	C23_015	melpomene	0	0	0	0	0	0	0	29	29
10_11_2023	3	South	Sunny	C23_195	cydno	0	0	0	0	0	0	0	29	29
10_11_2023	3	South	Sunny	C23_312	melpomene	0	0	0	0	0	0	0	29	29
10_11_2023	4	South	Cloudy	C23_407	cydno	2	0	0	0	2	0	2	0	29
10_11_2023	4	South	Cloudy	B23_970	melpomene	0	0	0	0	0	0	0	29	29
10_11_2023	5	South	Cloudy	C23_465	cydno	2	1	0	0	2	1	3	3	18
10_11_2023	5	South	Cloudy	C23_090	melpomene	6	8	0	0	6	8	14	7	0
10_11_2023	6	South	Cloudy	C23_215	cydno	3	0	0	0	3	0	3	1	29
10_11_2023	6	South	Cloudy	C23_327	melpomene	3	4	0	0	3	4	7	7	6
26_11_2023	1	South	Cloudy	C23_243	cydno	1	0	0	0	1	0	1	17	29
26_11_2023	1	South	Cloudy	C23_211	melpomene	5	5	0	4	5	9	14	0	15
26_11_2023	2	South	Cloudy	C23_215	cydno	0	0	0	0	0	0	0	29	29
26_11_2023	2	South	Cloudy	C23_146	melpomene	1	0	0	0	1	0	1	25	29
26_11_2023	3	South	Overcast	C23_193	cydno	0	0	0	0	0	0	0	29	29
26_11_2023	3	South	Overcast	B23_975	melpomene	0	0	0	0	0	0	0	29	29
28_11_2023	1	South	Overcast	C23_243	cydno	0	0	0	0	0	0	0	29	29
28_11_2023	1	South	Overcast	C23_305	melpomene	0	1	0	0	0	1	1	29	8
28_11_2023	2	South	Cloudy	C23_215	cydno	0	0	0	1	0	1	1	29	29
28_11_2023	2	South	Cloudy	C23_349	melpomene	0	0	0	0	0	0	0	29	29
28_11_2023	3	South	Overcast	C23_193	cydno	0	0	0	0	0	0	0	29	29
28_11_2023	3	South	Overcast	B23_874	melpomene	1	0	0	0	1	0	1	26	29
06_12_2023	1	South	Overcast	C23_609	cydno	2	0	0	2	2	2	4	1	29
06_12_2023	1	South	Overcast	B23_636	melpomene	2	1	1	0	3	1	4	21	15
06_12_2023	2	South	Overcast	C23_570	cydno	0	0	0	0	0	0	0	29	29
06_12_2023	2	South	Overcast	C23_576	melpomene	3	3	0	0	3	3	6	0	3
06_12_2023	3	South	Overcast	C23_585	cydno	0	0	0	0	0	0	0	29	29
06_12_2023	3	South	Overcast	C23_307	melpomene	0	1	0	0	0	1	1	29	11
06_12_2023	4	South	Overcast	C23_612	cydno	0	0	1	0	1	0	1	29	29
06_12_2023	4	South	Overcast	C23_472	melpomene	1	0	0	0	1	0	1	28	29
08_12_2023	1	North	Sunny	C23_485	cydno	0	0	0	0	0	0	0	29	29
08_12_2023	1	North	Sunny	C23_349	melpomene	0	0	0	0	0	0	0	29	29
08_12_2023	2	North	Sunny	C23_283	cydno	0	1	0	0	0	1	1	29	6
08_12_2023	2	North	Sunny	C23_331	melpomene	0	0	0	0	0	0	0	29	29
08_12_2023	3	North	Cloudy	C23_570	cydno	0	0	0	0	0	0	0	29	29
08_12_2023	3	North	Cloudy	C23_146	melpomene	0	0	0	0	0	0	0	29	29
08_12_2023	4	North	Cloudy	C23_609	cydno	0	0	0	0	0	0	0	29	29
08_12_2023	4	North	Cloudy	C23_039	melpomene	9	5	0	0	9	5	14	0	9
08_12_2023	5	North	Cloudy	C23_612	cydno	0	0	0	0	0	0	0	29	29
08_12_2023	5	North	Cloudy	C23_584	melpomene	0	0	0	0	0	0	0	29	29
09_12_2023	1	North	Overcast	C23_215	cydno	0	1	0	0	0	1	1	29	22
09_12_2023	1	North	Overcast	C23_468	melpomene	6	3	0	2	6	5	11	19	24
09_12_2023	2	North	Cloudy	C23_570	cydno	0	0	0	0	0	0	0	29	29
09_12_2023	2	North	Cloudy	C23_584	melpomene	0	0	0	0	0	0	0	29	29
12_12_2023	1	North	Sunny	C23_650	cydno	0	0	0	0	0	0	0	29	29
12_12_2023	1	North	Sunny	C23_649	melpomene	0	0	0	0	0	0	0	29	29
12_12_2023	2	North	Sunny	C23_609	cydno	0	0	0	0	0	0	0	29	29
12_12_2023	2	North	Sunny	C23_472	melpomene	1	0	0	0	1	0	1	17	29
12_12_2023	3	North	Sunny	C23_612	cydno	0	0	0	0	0	0	0	29	29
12_12_2023	3	North	Sunny	C23_146	melpomene	0	0	0	0	0	0	0	29	29
18_12_2023	1	North	Overcast	C23_681	cydno	0	0	0	0	0	0	0	29	29
18_12_2023	1	North	Overcast	C23_575	melpomene	0	0	0	0	0	0	0	29	29
18_12_2023	2	North	Overcast	C23_664	cydno	0	0	0	0	0	0	0	29	29
18_12_2023	2	North	Overcast	C23_525	melpomene	0	0	0	0	0	0	0	29	29
18_12_2023	3	North	Overcast	C23_650	cydno	0	0	0	0	0	0	0	29	29
18_12_2023	3	North	Overcast	C23_625	melpomene	1	0	1	0	2	0	2	9	29
19_12_2023	1	North	Cloudy	C23_612	cydno	0	0	0	0	0	0	0	29	29

19_12_2023	1	North	Cloudy	C23_584	melpomene	1	1	0	0	1	1	2	16	3
19_12_2023	2	North	Sunny	C23_609	cydno	0	0	0	0	0	0	0	29	29
19_12_2023	2	North	Sunny	C23_613	melpomene	1	1	0	0	1	1	2	13	12
19_12_2023	3	North	Overcast	C23_650	cydno	0	0	0	0	0	0	0	29	29
19_12_2023	3	North	Overcast	C23_704	melpomene	2	0	0	0	2	0	2	3	29
19_12_2023	4	North	Sunny	C23_664	cydno	0	0	0	0	0	0	0	29	29
19_12_2023	4	North	Sunny	C23_487	melpomene	1	1	0	0	1	1	2	21	19
19_12_2023	5	North	Cloudy	C23_681	cydno	0	0	0	0	0	0	0	29	29
19_12_2023	5	North	Cloudy	C23_306	melpomene	0	0	0	0	0	0	0	29	29
29_12_2023	1	North	Cloudy	C23_757	cydno	0	0	0	0	0	0	0	29	29
29_12_2023	1	North	Cloudy	C23_765	melpomene	0	0	0	0	0	0	0	29	29
29_12_2023	2	North	Cloudy	C23_754	cydno	0	1	0	0	0	1	1	29	3
29_12_2023	2	North	Cloudy	C23_719	melpomene	0	0	0	0	0	0	0	29	29
02_01_2024	1	North	Overcast	C23_755	cydno	0	0	0	0	0	0	0	29	29
02_01_2024	1	North	Overcast	C23_625	melpomene	0	2	0	0	0	2	2	29	12
02_01_2024	2	North	Overcast	C23_732	cydno	1	0	2	0	3	0	3	8	29
02_01_2024	2	North	Overcast	C23_792	melpomene	0	0	0	0	0	0	0	29	29
02_01_2024	3	North	Overcast	C23_826	cydno	0	0	0	0	0	0	0	29	29
02_01_2024	3	North	Overcast	C23_719	melpomene	2	0	0	0	2	0	2	0	29
02_01_2024	4	North	Overcast	C23_754	cydno	0	0	0	0	0	0	0	29	29
02_01_2024	4	North	Overcast	C23_744	melpomene	15	0	0	0	15	0	15	15	29
03_01_2024	1	North	Sunny	C23_609	cydno	0	0	0	0	0	0	0	29	29
03_01_2024	1	North	Sunny	C23_767	melpomene	1	1	0	0	1	1	2	11	9
03_01_2024	2	North	Sunny	C23_612	cydno	2	0	0	0	2	0	2	4	29
03_01_2024	2	North	Sunny	C23_613	melpomene	0	1	0	0	0	1	1	29	9
03_01_2024	3	North	Cloudy	C23_826	cydno	1	0	0	0	1	0	1	3	29
03_01_2024	3	North	Cloudy	C23_699	melpomene	0	2	0	0	0	2	2	29	27
03_01_2024	4	North	Cloudy	C23_754	cydno	0	0	0	0	0	0	0	29	29
03_01_2024	4	North	Cloudy	C23_584	melpomene	0	0	0	0	0	0	0	29	29
04_01_2024	1	South	Sunny	C23_755	cydno	1	1	0	0	1	1	2	4	21
04_01_2024	1	South	Sunny	C23_744	melpomene	0	1	0	0	0	1	1	29	1
04_01_2024	2	South	Sunny	C23_826	cydno	0	0	0	0	0	0	0	29	29
04_01_2024	2	South	Sunny	C23_559	melpomene	8	14	1	2	9	16	25	0	1
04_01_2024	3	South	Sunny	C23_612	cydno	2	0	0	0	2	0	2	1	29
04_01_2024	3	South	Sunny	C23_305	melpomene	0	0	0	0	0	0	0	29	29
04_01_2024	4	South	Sunny	C23_609	cydno	0	0	0	0	0	0	0	29	29
04_01_2024	4	South	Sunny	C23_765	melpomene	0	0	0	0	0	0	0	29	29
05_01_2024	1	South	Cloudy	C23_826	cydno	0	0	0	0	0	0	0	29	29
05_01_2024	1	South	Cloudy	C23_868	melpomene	0	2	0	0	0	2	2	29	10
05_01_2024	2	South	Cloudy	C23_865	cydno	1	0	0	0	1	0	1	14	29
05_01_2024	2	South	Cloudy	C23_311	melpomene	2	2	1	0	3	2	5	15	13
05_01_2024	3	South	Sunny	C23_755	cydno	2	0	0	0	2	0	2	21	29
05_01_2024	3	South	Sunny	C23_576	melpomene	0	0	0	0	0	0	0	29	29
05_01_2024	4	South	Cloudy	C23_612	cydno	0	0	0	0	0	0	0	29	29
05_01_2024	4	South	Cloudy	C23_559	melpomene	0	0	0	0	0	0	0	29	29
06_01_2024	1	South	Sunny	C23_755	cydno	0	0	0	0	0	0	0	29	29
06_01_2024	1	South	Sunny	C23_767	melpomene	0	0	0	0	0	0	0	29	29
06_01_2024	2	South	Cloudy	C23_826	cydno	0	0	0	0	0	0	0	29	29
06_01_2024	2	South	Cloudy	C23_613	melpomene	0	0	0	0	0	0	0	29	29
06_01_2024	3	South	Cloudy	C23_865	cydno	0	0	0	0	0	0	0	29	29
06_01_2024	3	South	Cloudy	C23_731	melpomene	0	0	0	0	0	0	0	29	29
06_01_2024	4	South	Overcast	C23_612	cydno	0	0	0	0	0	0	0	29	29
06_01_2024	4	South	Overcast	C23_791	melpomene	1	1	0	0	1	1	2	12	29
07_01_2024	1	South	Sunny	C23_865	cydno	0	0	0	0	0	0	0	29	29
07_01_2024	1	South	Sunny	C23_766	melpomene	4	0	0	0	4	0	4	15	29
07_01_2024	2	South	Sunny	C23_754	cydno	0	0	0	0	0	0	0	29	29
07_01_2024	2	South	Sunny	C23_704	melpomene	0	0	0	0	0	0	0	29	29
07_01_2024	3	South	Sunny	C23_826	cydno	1	1	0	0	1	1	2	22	3
07_01_2024	3	South	Sunny	C23_146	melpomene	1	0	0	0	1	0	1	27	29
08_01_2024	1	South	Sunny	C23_882	cydno	0	0	0	0	0	0	0	29	29
08_01_2024	1	South	Sunny	C23_719	melpomene	12	0	3	0	15	0	15	16	29
08_01_2024	2	South	Sunny	C23_755	cydno	0	0	0	0	0	0	0	29	29
08_01_2024	2	South	Sunny	C23_884	melpomene	5	0	0	0	5	0	5	2	29
08_01_2024	3	South	Sunny	C23_826	cydno	0	0	2	0	2	0	2	29	29
08_01_2024	3	South	Sunny	C23_883	melpomene	9	5	0	0	9	5	14	16	4
08_01_2024	4	South	Cloudy	C23_865	cydno	0	0	0	0	0	0	0	29	29
08_01_2024	4	South	Cloudy	C23_584	melpomene	0	1	0	0	0	1	1	29	29
08_01_2024	5	South	Cloudy	C23_754	cydno	0	0	0	0	0	0	0	29	29
08_01_2024	5	South	Cloudy	C23_894	melpomene	0	0	0	0	0	0	0	29	29
09_01_2024	1	South	Sunny	C23_732	cydno	0	0	0	0	0	0	0	29	29
09_01_2024	1	South	Sunny	C23_884	melpomene	0	5	0	0	0	5	5	29	2
09_01_2024	2	South	Cloudy	C23_755	cydno	1	0	0	0	1	0	1	13	29
09_01_2024	2	South	Cloudy	C23_625	melpomene	0	0	0	0	0	0	0	29	29
09_01_2024	3	South	Overcast	C23_754	cydno	0	0	0	0	0	0	0	29	29
09_01_2024	3	South	Overcast	C23_744	melpomene	1	0	0	0	1	0	1	9	29
11_01_2024	1	South	Cloudy	C23_882	cydno	0	0	0	1	0	1	1	29	29

11_01_2024	1	South	Cloudy	C23_894	melpomene	0	1	0	0	0	1	1	29	21
11_01_2024	2	South	Cloudy	C23_826	cydno	0	0	0	0	0	0	0	29	29
11_01_2024	2	South	Cloudy	C23_745	melpomene	8	4	1	1	9	5	14	15	8
11_01_2024	3	South	Cloudy	C23_919	cydno	0	0	0	1	0	1	1	29	29
11_01_2024	3	South	Cloudy	C23_928	melpomene	0	0	0	0	0	0	0	29	29
11_01_2024	4	South	Overcast	C23_732	cydno	0	0	0	0	0	0	0	29	29
11_01_2024	4	South	Overcast	C23_910	melpomene	0	0	0	0	0	0	0	29	29
12_01_2024	1	South	Sunny	C23_882	cydno	0	0	0	0	0	0	0	29	29
12_01_2024	1	South	Sunny	C23_928	melpomene	3	0	0	0	3	0	3	18	29
12_01_2024	2	South	Cloudy	C23_732	cydno	0	0	0	0	0	0	0	29	29
12_01_2024	2	South	Cloudy	C23_952	melpomene	0	0	0	0	0	0	0	29	29
12_01_2024	3	South	Overcast	C23_755	cydno	2	0	1	2	3	2	5	9	29
12_01_2024	3	South	Overcast	C23_883	melpomene	0	0	0	0	0	0	0	29	29
12_01_2024	4	South	Overcast	C23_754	cydno	0	0	0	0	0	0	0	29	29
12_01_2024	4	South	Overcast	C23_865	melpomene	0	0	0	0	0	0	0	29	29
16_01_2024	1	South	Sunny	C23_914	cydno	0	0	0	0	0	0	0	29	29
16_01_2024	1	South	Sunny	C23_928	melpomene	2	2	0	0	2	2	4	9	27
16_01_2024	2	South	Sunny	C23_732	cydno	0	0	0	0	0	0	0	29	29
16_01_2024	2	South	Sunny	C23_883	melpomene	0	0	0	0	0	0	0	29	29
16_01_2024	3	South	Sunny	C23_755	cydno	0	0	0	0	0	0	0	29	29
16_01_2024	3	South	Sunny	C23_884	melpomene	0	0	0	0	0	0	0	29	29
16_01_2024	4	South	Sunny	C23_920	cydno	0	0	0	0	0	0	0	29	29
16_01_2024	4	South	Sunny	C23_719	melpomene	0	0	0	0	0	0	0	29	29
16_01_2024	5	South	Sunny	C23_754	cydno	0	0	0	0	0	0	0	29	29
16_01_2024	5	South	Sunny	C23_744	melpomene	0	1	0	0	0	1	1	29	14
17_01_2024	1	South	Sunny	C23_732	cydno	1	0	0	0	1	0	1	12	29
17_01_2024	1	South	Sunny	C23_883	melpomene	0	0	0	0	0	0	0	29	29
17_01_2024	2	South	Sunny	C23_972	cydno	0	0	0	0	0	0	0	29	29
17_01_2024	2	South	Sunny	C23_952	melpomene	2	0	0	0	2	0	2	3	29
17_01_2024	3	South	Sunny	C23_754	cydno	0	0	1	0	1	0	1	29	29
17_01_2024	3	South	Sunny	C23_776	melpomene	1	0	0	0	1	0	1	11	29
17_01_2024	4	South	Sunny	C23_914	cydno	0	0	0	0	0	0	0	29	29
17_01_2024	4	South	Sunny	C23_305	melpomene	0	0	0	0	0	0	0	29	29
18_01_2024	1	South	Sunny	C23_972	cydno	0	0	0	0	0	0	0	29	29
18_01_2024	1	South	Sunny	C23_910	melpomene	0	0	0	0	0	0	0	29	29
18_01_2024	2	South	Sunny	C23_732	cydno	0	0	0	0	0	0	0	29	29
18_01_2024	2	South	Sunny	C23_625	melpomene	0	0	0	0	0	0	0	29	29
18_01_2024	3	South	Sunny	C23_754	cydno	0	0	0	0	0	0	0	29	29
18_01_2024	3	South	Sunny	C23_487	melpomene	0	0	0	0	0	0	0	29	29

Table S6| Data from the obstacle avoidance experiment.

TS: time to cross in simple (3RPM) treatment.

TF: time to cross in simple (18RPM) treatment.

Numbers 1-3 indicate replicate number.

Male	**Species**	**TS1**	**TF1**	**TS2**	**TF2**	**TS3**	**TF3**
C23_507	C	1.0	1.2	1.3	1.45	1.3	1.1
C23_491	M	2.6	2.1	2.9	2.3	2.9	1.7
C23_243	C	1.6	2.2	1.5	2.3	2.1	4.8
C23_307	M	1.4	1.8	1.9	2.0	1.9	1.8
C23_506	C	3.1	1.8	2.2	5.3	3.8	1.4
C23_184	M	1.2	3.6	2.1	2.9	1.9	1.4
C23_710	C	3.7	2.1	1.9	2.3	2.7	3.9
C23_446	M	2.0	1.65	3.0	2.1	2.4	NA
C23_485	C	1.4	2.4	2.2	3.0	1.1	3.0
C23_349	M	1.7	3.56	1.8	2.5	2.6	1.6
C23_069	C	2.6	4.0	3.6	3.5	1.85	1.6
C23_487	M	2.2	1.8	4.4	2.5	3.8	2.4
C23_283	C	1.3	2.2	1.8	2.3	2.8	3.4
C23_910	M	2.1	2.5	1.8	1.8	1.4	1.9
C23_193	C	3.1	1.4	1.4	1.7	1.8	1.5
C23_306	M	4.9	3.1	1.8	2.1	3.8	1.9
C23_112	C	1.7	1.1	1.2	2.1	1.4	1.7

C23_894	M	3.1	2.1	1.8	2.9	1.9	1.7
C23_305	M	1.9	2.2	1.5	2.3	1.9	2.7



Figure S1 | Rotary obstacle apparatus as seen from the dark chamber of the experimental insectary. Top: modified optomotor machine. Left and right: opaque divider within the insectary, forming a bright slit.

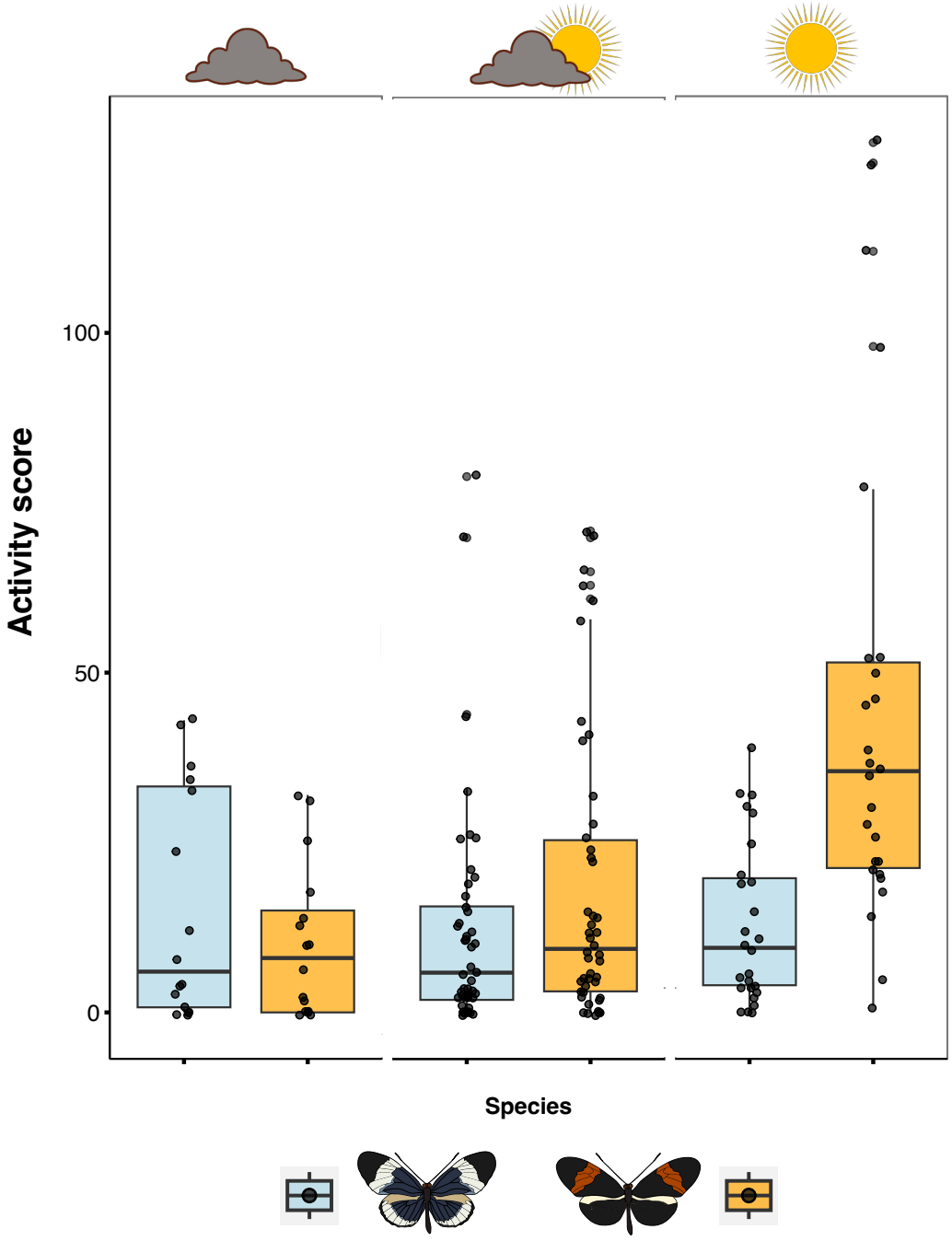


Figure S2 | Weather had a significant effect on the activity of the butterflies. Specifically, butterflies were more active during sunny trials (right) than during cloudy (middle) or overcast (left) trials.

Last page of the master's thesis (including statement of originality)

This form must be filled out and is to be included as the last page in the printed copy of your master's thesis for the Examination Committee.
Dieses Formblatt ist ausgefüllt als letzte Seite in das beim Prüfungsausschuss abzugebende Exemplar der Masterarbeit einzubinden.

Last name, first name: _____

Signature of the (internal) supervisor: _____

Starting date of the master's thesis: _____

Submission date of the master's thesis: _____

Master's thesis statement of originality

I hereby confirm that I have written the accompanying thesis myself, without contributions from any sources other than those cited in the text and acknowledgements. This applies also to all graphics, drawings, maps and images included in the thesis.

Erklärung zur Masterarbeit

Hiermit versichere ich, dass die vorliegende Arbeit von mir selbstständig verfasst wurde und dass keine anderen als die angegebenen Quellen und Hilfsmittel benutzt wurden. Diese Erklärung erstreckt sich auch auf in der Arbeit enthaltene Graphiken, Zeichnungen, Kartenskizzen und bildliche Darstellungen.

_____ _____

Place, date
Ort, Datum

Signature
Unterschrift